The Effect of Acute Intermittent Hypercapnia and Exercise on Ventilatory Chemosensitivity and Cardiovascular Function

by

Paige J. Rynne

A thesis

presented to the University of Waterloo

in fulfillment of the

thesis requirement for the degree of

Master of Science

in

Kinesiology

Waterloo, Ontario, Canada, 2025

© Paige J. Rynne 2025

Author's Declaration

I hereby declare that I am the sole author of this thesis. This is a true copy of the thesis, including any required final revisions, as accepted by my examiners.

I understand that my thesis may be made electronically available to the public.

Abstract

Ventilatory long-term facilitation (vLTF) is a form of respiratory plasticity triggered by intermittent hypoxia (IH) in the presence of CO_2 (1,2,4,34). The manifestation of vLTF following intermittent hypercapnia (IHc) without concurrent hypoxia – particularly in combination with exercise- remains unclear. This study evaluated the physiological effects of IHc and moderate-intensity exercise on cardiovascular function and ventilatory control in the resting and exercising states. Twenty healthy participants (10F) completed a three-visit protocol, including two experimental exposures to either IHc ($P_{ET}CO_2$ +5mmHg for 40s, intersped with 20s normocapnic normoxia) or continuous room air (control), each followed by an exercising and resting observational period (~45 minutes in total). At rest, the cardiovascular response to IHc was not found to be different from control. During exercise, heart rate (HR) increased following IHc and mean arterial pressure (MAP) significantly decreased (HR: +12bpm, $p < 0.001$; MAP: -8mmHg, $p = 0.006$), while both appeared stable in the time-matched control. Exercising peripheral hypercapnic chemosensitivity (PHC) appeared constant over time with IHc (+14 ± 25%), contradicting the significant decrease observed with control (-8 ± 20%, $p = 0.017$). While ventilation ($\dot{V}_E$) increased across both states following IHc relative to control, only resting $\dot{V}_E$ was disproportionate to metabolic demand, as reflected by a lower $\%\Delta\dot{V}_E/\%\Delta\dot{V}CO_2$ ratio relative to control. These findings suggest the presence of exercise with IHc may have a modulatory role in the development or expression of cardiorespiratory plasticity, as well as implicating sensory long-term facilitation (LTF) as a contributor to vLTF. Finally, a progressive amplification in $\dot{V}_E$ over the course of IHc, independent of CO_2 stimulus intensity, is consistent with early-stage chemosensory gain. Collectively, these findings demonstrate that IHc without hypoxia can elicit key indicators of vLTF.

Acknowledgements

First and foremost, I would like to thank all the participants who volunteered to take part in my study and made this work possible.

I would also like to thank my supervisor Paolo Dominelli for giving me the opportunity to conduct this research, for the amount of knowledge he shared (although not all of it stuck), and for the support he offered along the way. To my committee, Jason Au, Michaela Devries-Aboud, and Glen Foster, thank you for contributing your time and expertise to this research.

To my lab mates, Allie Pulford-Thorpe, Armando Aguero, Leah Mann, Victoria Chang, Ben Thompson, Sarah Angus, and Connor Doughtery – thank you for always being willing to help, whether it be to offer a hand or an explanation, and for consistently making the lab a fun environment.

To my family and Matina, thank you for your unwavering support, and for always pretending to understand when I explained my research to you.

Finally, I would like to thank my dog Casper, for always keeping me company during this process, and for keeping my feet warm while I wrote.

Table of Contents

Author's Declaration ii

Abstract iii

Acknowledgements iv

List of Figures viii

List of Tables ix

List of Equations x

List of Abbreviations xi

Chapter 1 Literature Review 1

1.1 Introduction to the Literature Review 1

1.2 Overview of the Control of Ventilation 2

1.2.1 Peripheral Control of Ventilation 3

1.2.2 Central Control of Ventilation 4

1.3 The Effect of Hypoxia on the Control of Ventilation and Cardiovascular Function 5

1.4 The Effect of Hypercapnia on the Control of Ventilation and Cardiorespiratory Function 6

1.5 The Effect of Intermittent Hypoxia on Ventilatory Chemosensitivity and Cardiovascular Function 7

1.6 Intermittent Hypercapnia and Cardiovascular Function 10

1.7 The Effect of Exercise on the Cardiorespiratory System 13

1.8 The Effect of Exercise on the Respiratory Chemoreflex 13

Chapter 2 Study Rationale 15

Chapter 3 Research Questions and Hypotheses 17

Chapter 4 Methods 18

4.1 Ethics 18

4.2 Participants 18
4.3 Experimental Overview 19
4.3.1 Day Day One: Screening, $\dot{V}O_{2max}$ Testing, and Air Force Familiarization 20
4.3.2 Day 2 and 3: Experimental Protocol 21
4.3.3 PHC Testing 24
4.4 Data Collection 25
4.4.1 Cardiorespiratory Measurements 25
4.4.2 Dynamic End-Tidal Forcing 27
4.5 Data Analysis 27
4.5.1 Cardiorespiratory Parameters 27
4.5.2 Maximal Exercise Capacity 28
4.5.3 PHC Testing 28
4.6 Statistical Analysis 29
4.6.1 Cardiorespiratory Function 32
4.6.2 PHC Statistical Analysis 32
Chapter 5 Results 34
5.1 Participant Demographics, Baseline Values & Maximal Exercise Testing 34
5.2 Cardiovascular Responses at Rest 35
5.3 Cardiovascular Responses during Exercise 38
5.4 The Control of Ventilation at Rest 41
5.5 The Control of Ventilation during Exercise 43
5.6 Changes in Resting PHC 46
5.7 Changes in Exercising PHC 49
5.8 Acute Responses to IHc 52

5.8.1 Cha nges During 40s vs 20s Cycles Between Conditions 54

5.8.2 Changes from the First to Last 5- Minutes during IHc and Control 57

5.8.3 Differences in the Magnitude of Response to Hypercapnia (Δ40s-20s) over the course of IHc 60

Chapter 6 Discussion 62

6.1 Main Findings 62

6.2 Implications for Cardiovascular Regulation 63

6.2.1 Blood Pressure and Autonomic Modulation 63

6.2.2 Evidence for Sympathetic LTF 65

6.3 The Impact of IHc and Exercise on Ventilatory Control and Plasticity 66

6.3.1 Primary Indicators of Sensory LTF 66

6.3.2 Secondary Evidence for Sensory LTF 66

6.4 Differences in Cycle-Driven Effects between Conditions 69

6.4.1 Acute Effects During 40s vs 20s Cycles Between Conditions 70

6.4.2 Time -Dependent Changes Across the First and Last 5-Minutes (Between Conditions) 71

6.4.3 Phasic Amplification of the Acute Hypercapnic Response Over Time (Within IHc only) 72

Chapter 7 Perspectives 73

Chapter 8 Considerations and Limitations 75

Chapter 9 Conclusion 77

References 78

List of Figures

Figure 1. Major influences of autonomic respiratory control 2

Figure 2. Potential locations and types of plastic enhancements occurring within peripheral chemoreceptor feedback loop 10

Figure 3. Pathways in which IHc may lead to plastic changes facilitating ventilatory and autonomic function. 12

Figure 4. Schematic of overall study protocol 20

Figure 5. An example of raw data for a participant during IHc 23

Figure 6. Day 2 and 3 protocol overview 23

Figure 7. Schematic of the rebreathing system used day 2 and 3 of testing 24

Figure 8. Experimental instrumentation and set up for cardiovascular measurements 26

Figure 9. Data acquisitions software showing an example of PHC testing 29

Figure 10. An example of one participant's raw data across IHc and control with important time groupings and events highlighted 31

Figure 11. Average ± SD resting HR and BP across time and conditions 37

Figure 12. Average ± SD exercising HR and BP across time and conditions 40

Figure 13. Average ± SD ventilation, breathing frequency, and tidal volume at rest across time and conditions. 43

Figure 14. Average ± SD ventilation, breathing frequency, and tidal volume across time and conditions during exercise 46

Figure 15. Average ± SD resting PHC, $\Delta P_{ET}CO_2$, and $\Delta \dot{V}_E$ across time and conditions 49

Figure 16. Average ± SD exercising PHC, $\Delta P_{ET}CO_2$, and $\Delta \dot{V}_E$ across time and conditions 52

Figure 17. Overview of analytical comparisons made to evaluate acute responses to IHc 53

Figure 18. Mean ± SD percent change from 20s to 40s cycles by condition 57

Figure 19. Mean ± SD percent change from the first to last 5 minutes of condition 60

Figure 20. Changes in $\Delta \dot{V}_E$ and $\Delta P_{ET}CO_2$ in response to hypercapnic cycles over the course of IHc 61

List of Tables

Table 1. Participant inclusion and exclusion criteria 19

Table 2. Participant demographics and maximal exercise test results 34

Table 3. Baseline resting and exercising measurements between conditions 35

Table 4. Average resting cardiovascular responses across time and conditions 36

Table 5. Average exercising cardiovascular measurements across time and conditions 39

Table 6. Average resting ventilatory activity across time and conditions 42

Table 7. Average exercising ventilatory activity in room air across time and conditions 45

Table 8. Average ventilatory output during 20s of baseline (pre-stimulus) and in response to PHC trials Pre and Post condition at rest 48

Table 9. Average exercising ventilatory output during 20s of baseline (pre-stimulus) and in response to PHC testing across time and conditions 51

Table 10. Acute changes in cardiorespiratory activity between 40s and 20s cycles during IHc and control 56

Table 11. Average ± SD cardiorespiratory activity over the course of the first and last 5 minutes by condition 59

List of Equations

Equation 1. $P_aCO_2 = \frac{VCO_2}{V_A} \times K$

List of Abbreviations

$\dot{V}_A$	Alveolar ventilation
ANOVA	Analysis of variance
P_aO_2	Arterial partial pressure of oxygen
P_aCO_2	Arterial partial pressure of carbon dioxide
BP	Blood pressure
BMI	Body mass index
BTPS	Body temperature pressure saturated
CB	Carotid body
CO_2	Carbon dioxide
$\dot{V}CO_2$	Carbon dioxide output
$\dot{Q}$	Cardiac output
CSF	Cerebral spinal fluid
DBP	Diastolic blood pressure
ETF	End-tidal forcing
f_B	Frequency of breathing
HR	Heart rate
HVR	Hypoxic ventilatory response
HVD	Hypoxic ventilatory decline
IHc	Intermittent hypercapnia
IHH	Intermittent hypercapnic hypoxia
IH	Intermittent hypoxia
LTD	Long-term depression
LTF	Long-term facilitation
HR_{max}	Maximal heart rate
MWR	Maximal work rate
MAP	Mean arterial pressure
mmHg	Millimeters of mercury
$\dot{V}_I$	Minute ventilation
NTS	Nucleus tractus solitarii
O_2	Oxygen
OSA	Obstructive sleep apnea
$\dot{V}O_2$	Oxygen uptake
S_PO_2	Oxyhemoglobin saturation
PCO_2	Partial pressure of carbon dioxide
PO_2	Partial pressure of oxygen
$\dot{V}O_{2max}$	Maximal oxygen consumption
RER	Respiratory exchange ratio
SBP	Systolic blood pressure
sLTF	Sensory long-term facilitation
SNA	Sympathetic nerve activity
SV	Stroke volume
V_T	Tidal volume
$\dot{V}_E$	Ventilation
vLTF	Ventilatory long-term facilitation

Chapter 1
Literature Review

1.1 Introduction to the Literature Review

Peripheral chemoreceptor input fine tunes resting ventilatory drive and influences cardiovascular function. With exercise and stimuli such as hypoxia or hypercapnia, peripheral chemoreceptor sympathetic outflow to the brain increases, ultimately leading to a rise in ventilation ($\dot{V}_E$) and cardiac output ($\dot{Q}$). In cases where hypoxia follows a cyclical pattern, termed intermittent hypoxia (IH), elevations in sympathetic outflow and arterial blood pressure (BP) last minutes to hours following the exposure (1). Enhancements in neural plasticity cause resting $\dot{V}_E$ to remain elevated following the IH exposure, known as ventilatory long-term facilitation (vLTF)(2–4). Increases in respiratory chemosensitivity to hypoxia occur following IH, and similar changes in peripheral hypercapnic chemosensitivity (PHC) are observed when IH is paired with sustained or intermittent hypercapnia (IHc) (1,5,6).

The presence and control of carbon dioxide (CO_2) influences mechanisms related to the facilitation of sympathetic activity (1,6). A study which isolated the effects of IHc on cardiorespiratory function found a decrease in $\dot{V}_E$ and the facilitation of arterial BP, which lasted beyond the IHc protocol (7). The current study aims to evaluate changes in respiratory chemosensitivity as a possible mechanism for cardiorespiratory adjustments following IHc. Furthermore, exercise is a powerful stimuli in augmenting $\dot{V}_E$, BP, and peripheral chemosensitivity to oxygen (O_2) and CO_2 challenges (8,9). Therefore, this study will utilize exercise as an additional stimulus to investigate whether an active state influences cardiorespiratory adaptations and underlying mechanisms manifesting following IHc.

1.2 Overview of the Control of Ventilation

In order to maintain optimal concentrations of arterial O_2 and CO_2, $\dot{V}_E$ is tightly regulated with metabolic demand. The regulation is achieved through the integration of several synergistic feedforward and feedback mechanisms. An important feedback loop involved in the control of breathing is the ventilatory chemoresponse, which involves the integration of afferent activity by peripheral and central chemosensors regarding blood and cerebral spinal fluid (CSF) gas pressures, respectively. Respiratory control centers in the medulla are responsible for integrating afferent feedback and generating efferent signals which, in turn, trigger an adjustment to $\dot{V}_E$ through changes in breath frequency and depth. Other factors influencing $\dot{V}_E$ include feedback from peripheral sensory nerves in the muscles and lungs, and feedforward mechanisms such as the central pattern generator within the brainstem. During rest at low altitude, the chemoresponse fine tunes $\dot{V}_E$ and is not the principal pattern generator (10). Figure 1 provides a visual overview of the major influences on autonomic respiratory control pertaining to this study.

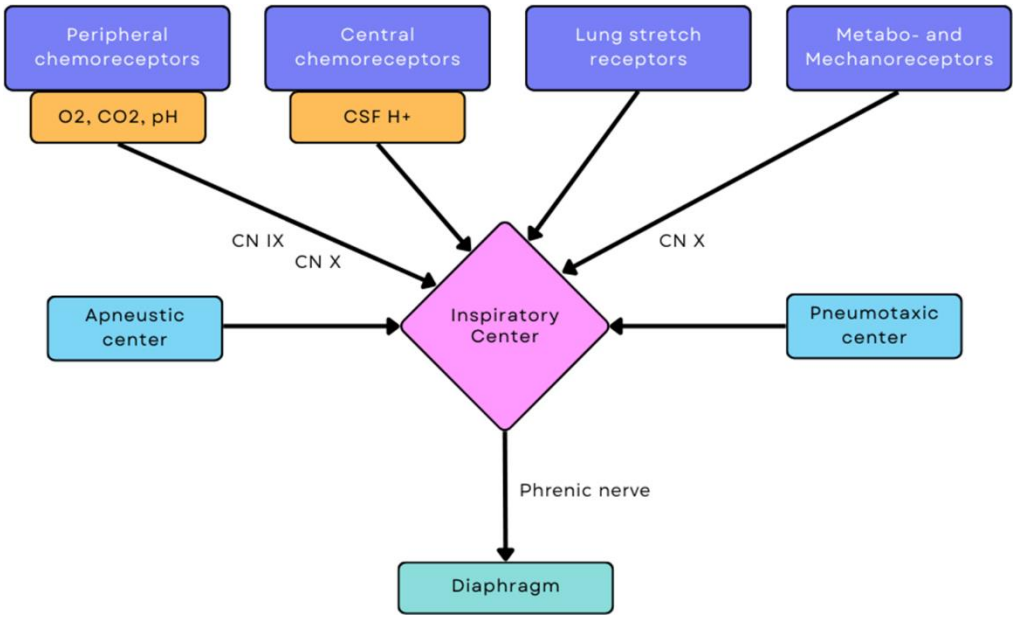


Figure 1. Major influences of autonomic respiratory control. CO_2, carbon dioxide; CN IX, glossopharyngeal nerve; CN X, vagus nerve; CSF H^+, cerebral spinal fluid hydrogen ion content; O_2, oxygen.

1.2.1 Peripheral Control of Ventilation

There are two types of peripheral chemoreceptors. Aortic chemoreceptors are located along the aortic arch and communicate with the medulla via the vagus nerve (cranial nerve X). Carotid chemoreceptors are located at the bifurcation point of the common carotid arteries into the internal and external carotid arteries. These chemoreceptors communicate with the medulla via the carotid sinus nerve (CSN), a branch of the glossopharyngeal nerve (cranial nerve IX), and play a more significant role than aortic chemoreceptors in the control of breathing. The carotid bodies are polymodal, as they are sensitive to blood gases and several other blood-borne stimuli including temperature, K+, and glucose (11). Carotid chemoreceptors contain glomus type 1 cells which are sensitive to decreases in arterial blood pH and O_2 pressure and increases in arterial CO_2 pressure (12). When these conditions are detected, glomus type 1 cells depolarize and release neurotransmitters causing increased afferent firing along the CSN to the medulla. Carotid body (CB) discharge increases exponentially as the partial pressure of arterial O_2 (PaO_2) decreases (13,14). In the case of excess arterial O_2, a condition known as hyperoxia, afferent discharge is inhibited, although it is never fully abolished (14). From the CSN, the afferent signal is transmitted to the nucleus tractus solitarii (NTS) located at the base of the medulla. The signal is passed to a series of respiratory control centers within the medulla where it is integrated to generate an efferent output to adjust respiratory muscle activity accordingly. The primary efferent pathway is the phrenic motor neuron, which innervates the diaphragm.

Activation of the CB also results in cardiovascular system modulation. Upon chemoreceptor stimulation, peripheral vasoconstriction and bradycardia occur (13,15). However, as CB activation persists, the increase in respiratory drive and activation of pulmonary stretch receptors from hyperventilation leads to an increase in vagal afferent activity, resulting in tachycardia and peripheral

vasoconstriction (13,15). Therefore, the cardiovascular effects of CB stimulation are heavily influenced by contaminant baroreceptor stimulation.

1.2.2 Central Control of Ventilation

Central chemoreceptors are located within several regions of the medulla and are known to be sensitive to fluctuations in CSF hydrogen ion [H+] concentrations. The status of brain interstitial fluid provides insight into alveolar ventilation ($\dot{V}_A$), acid-base balance, metabolism, and brain blood flow. Central chemoreceptor input prompts the adjustment of $\dot{V}_E$ and airway resistance in response to variations in CSF pH as a protective mechanism for brain tissue (16). Studies have generalized that a 1.5 mmHg increase in alveolar PCO_2 causes $\dot{V}_E$ to approximately double in a healthy population (17).

However, due to the time required for gas diffusion into the brainstem, central chemoreceptors are delayed in comparison to peripheral chemoreceptors. Central chemoreceptor activation occurs approximately 50 seconds after the onset of a hypercapnic stimulus (18). The lag in detection has been attributed to prolonged equilibration time of CSF [H+] to changes in partial pressures of arterial CO_2 ($PaCO_2$), a delay which prevents central chemoreceptors from sensing acute changes in $PaCO_2$.

Central chemoreceptor input also contributes to adjustments in cardiac function through sympathetic tone modulations, an additional protective mechanism to counteract fluctuations in CSF pH. These adjustments are seen as elevations in BP, and modulation of $\dot{Q}$ and blood flow to various organs (18). It is believed that changes in cardiac function are secondary to, and highly dependent on, the initial ventilatory response to central chemoreceptor input (18).

1.3 The Effect of Hypoxia on the Control of Ventilation and Cardiovascular Function

Hypoxia refers to a decreased partial pressure of O_2 (PO_2) in inspired air, thereby leading to hypoxemia, a state of decreased PaO_2. Hypoxemia is promptly sensed by peripheral chemoreceptors, and results in an increased respiratory drive to increase $\dot{V}_E$. Referred to as the hypoxic ventilatory response (HVR), this process occurs within seconds of the onset of hypoxia. With an increase in $\dot{V}_E$, there is a coinciding decrease in arterial CO_2 tension. Hypoxic ventilatory depression (HVD) is observed in awake humans 5-30 minutes following the onset of isocapnic hypoxia, whereby there is a blunting of respiratory drive and phrenic nerve activity (19,20). Ventilatory acclimatization is observed as an increase in $\dot{V}_E$, primarily achieved through an increase in breathing frequency (f_B) and can last from hours to weeks following removal from a hypoxic environment. However, research has shown that the duration, dose, and pattern of hypoxic exposure plays a significant role in the manifestation of physiological adaptations.

Cardiovascular function must increase in acute hypoxia to meet tissue perfusion demands in compensation for the decreased arterial oxygen concentration (21). Upon the onset of hypoxia, heart rate (HR), and $\dot{Q}$ rise via β-adrenergic stimulation (22). Peripheral vasoconstriction occurs to direct blood flow towards vital organs such as the heart and brain (21). Despite the increase in $\dot{Q}$, stroke volume (SV) remains largely unchanged (23). BP is also maintained in acute hypoxia, as sympathetic global vasoconstriction counteracts the dilation of peripheral vascular beds (23). The observed cardiovascular changes in acute hypoxia are attributed primarily to an increase in sympathetic neural discharge, and are related to the severity of hypoxia (21).

1.4 The Effect of Hypercapnia on the Control of Ventilation and Cardiorespiratory Function

Hypercapnia is defined as an elevation in $PaCO_2$ above baseline caused by inadequate $\dot{V}_E$. $PaCO_2$ is tied to the rate of CO_2 production ($\dot{V}CO_2$) and $\dot{V}_A$, a relationship best explained by the alveolar ventilation equation (*Equation 1*). Hypercapnia can be caused by an accumulation of CO_2 as a metabolic by-product due to hypoventilation, apnea (through loss of consciousness or conditions such as sleep apnea), lung diseases, or through environmental exposures such as rebreathing expired air.

Equation 1:

$$P_aCO_2 = \frac{\dot{V}CO_2}{\dot{V}_A} \times K$$

Where $PaCO_2$ = partial pressure of carbon dioxide in arterial blood, $\dot{V}CO_2$ = volume of carbon dioxide production, $\dot{V}_A$ = alveolar ventilation, and K= ideal gas law constant (863 mmHg).

Hyperventilation is observed upon the onset of hypercapnia. A linear relationship has been found between chemoreceptor activity and carbon dioxide tension in acute hypercapnic exposures (24). Research investigating the prolonged effect of hypercapnia (3.5% CO_2 for 10 days) has shown desensitization of the peripheral chemoresponse with an increase in central chemosensitivity, although this was in a cane toad model (25).

Mild hypercapnia (<+2 mmHg PaCO2) increases $\dot{Q}$ due to the activation of sympathoadrenal processes and sympathetic tone, as well as increases in preload, HR, capacitance, and venous return (26). In a mildly hypercapnic state, a 60% increase in $\dot{Q}$ has been observed despite a 10-20% increase in O_2 consumption ($\dot{V}O_2$)(24). These findings reveal the stimulatory effect of CO_2, as the increase in cardiac function was not solely caused by an increase in O_2 demand. Others found an increase in

circulating catecholamines (epinephrine and norepinephrine) following a hypercapnic exposure of 7-15% CO_2 (24).

When exercising at an intensity below ventilatory threshold, breathing 3% CO_2 (21% O_2, balance N_2) causes an increase in $\dot{V}_E$ in comparison to room air or HeO_2 (79% He, 21% O_2) (27). There is a dose-dependent increase in $\dot{V}_E$ with increasing inspired CO_2 concentration despite a decrease in self-paced endurance exercise performance (28). Similarly, exercise and hypercapnia have an additive stimulatory effect on the cardiovascular system. A study by Moriyama et al. (2022) exposed participants to hypercapnia (6% CO_2, 21% O_2) during steady state exercise and observed an increase in MAP, HR, and $\dot{Q}$ in comparison to normoxic exercise (29).

Limited research has evaluated hypercapnic exercise and respiratory chemosensitivity. A study which subjected participants to 3% CO_2 for 6-minutes while cycling at a moderate intensity found hypercapnic chemosensitivity was enhanced in comparison to exercise done in room air (9). They concluded that hypercapnic exercise augmented $\dot{V}_E$ in a manner suggestive of vLTF (9). It is important to note that given the length of hypercapnic exposure used by Yamashiro et al., central chemoreceptors likely played a role in $\dot{V}_E$ augmentation. No studies have utilized a hypercapnic protocol to isolate peripheral chemoreceptor stimulation during exercise.

1.5 The Effect of Intermittent Hypoxia on Ventilatory Chemosensitivity and Cardiovascular Function

The manifestation of vLTF following IH is characterized as an increase in resting $\dot{V}_E$ that occurs primarily through an increase in tidal volume (V_T). IH causes an increased expression of presynaptic neuropeptides, which in time enhances synaptic plasticity and leads to a form of behavioral sensitization as the increase in respiratory motor output outlasts the initiating stimulus. Ventilatory plastic enhancements are dependent on IH duration, dose, pattern, and exposure history,

and has been found to last from minutes to days following the cessation of IH (3). It is believed that an increase in respiratory chemosensitivity is involved in the observed increase in respiratory drive. The exact location of the enhancements along the chemosensitivity feedback loop has been at the speculation of many researchers, with evidence supporting both controller gain - an increase in afferent signaling for a given blood gas concentration, and plant gain - an increased change in blood gas concentration for a given change in $\dot{V}_E$. The CB was thought to be primarily responsible for the enhancements in neural plasticity. However, rats which had undergone CB denervation to IH and found vLTF still manifested, but to a lesser extent, which is indicative of synaptic plasticity enhancements at additional locations within the respiratory feedback loop (30,31). Similarly, vLTF occurring following intermittent hypercapnic hypoxia (IHH) is augmented via hyperoxia-induced peripheral chemoreceptor blunting, but not abolished (1). Further research has proposed that facilitation may occur along the carotid sinus nerve, within central respiratory cent, or within phrenic motor nuclei (1,2). Figure 2 visualizes the different potential locations and types of plastic enhancements which have been found to occur within peripheral chemoreceptor feedback loop.

The increase in ventilatory chemosensitivity following IH seems to be exposure specific. Others showed an increased HVR following IH saw no changes in the hypercapnic ventilatory response (HCVR) (32). Furthermore, the presence of exercise does not seem to influence HCVR sensitivity following IH. Individuals who underwent hyperbaric hypoxia for 30 minutes/day on 6 consecutive days while exercising or at rest, experienced no change in HCVR between conditions (33). However, when IH is paired with hypercapnia, increases in tonic CB activity post-exposure are evident (1,6).

The presence of CO_2 during hypoxic exposures plays an important role in the manifestation of vLTF. For example, IH paired with isocapnia or poikilocapnia does not cause the manifestation of

vLTF (2,4,34). These studies concluded that hypercapnia must be sustained throughout the duration of IH and recovery to observe enhancements in neural plasticity. A recent study challenged this by evaluating the effects of intermittent hypercapnic hypoxia (IHH) paired with isocapnic-normoxic recovery (1). It was found that IHH elicited vLTF, despite the absence of elevated CO_2 during recovery (1). These findings are suggestive that intermittent exposures to CO_2 may influence tonic peripheral chemoreceptor drive.

A large increase in sympathetic outflow can be observed following IH and attributes to increases in $\dot{V}_E$ and cardiac function. Sustained elevations in MAP via upregulation of RAAS is corroborated by research which utilized a pharmacological angiotensin-II type 1 receptor blockade to abolish BP increases following 6-hours of IH (35). The increase in MAP is largely attributed to elevations in diastolic blood pressure (DBP) (1). Subjecting participants to 1 hour of IH (SpO_2 ~ 80%) for 10 consecutive days caused an increase in sympathetic outflow during and following IH, which was sustained beyond $\dot{V}_E$, BP, and SpO_2 returning to baseline levels (36). Importantly, the increased sympathetic activity was closely correlated with the HVR, which was also increased in comparison to baseline following IH. Changes in BP sensitivity following IH have also been found to be closely related to changes in the HVR (32). Despite these sympathetic increases, HR remains unchanged following IH (37).

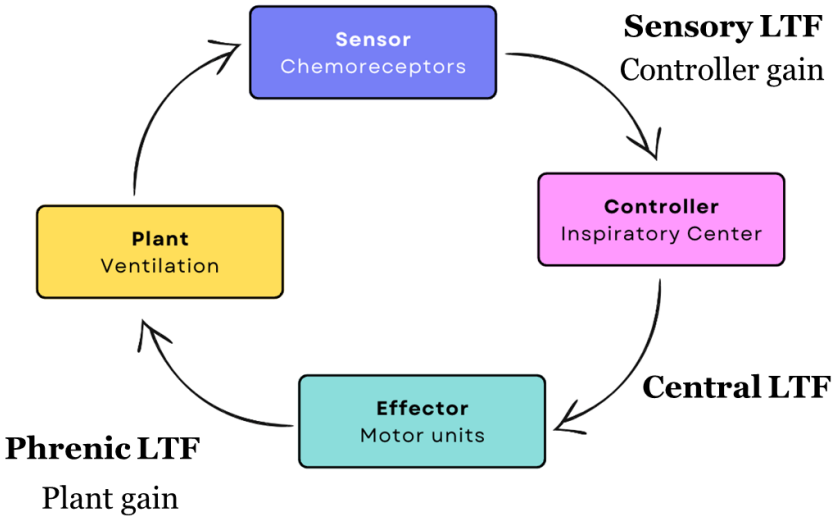


Figure 2. Potential locations and types of plastic enhancements occurring within peripheral chemoreceptor feedback loop.

1.6 Intermittent Hypercapnia and Cardiovascular Function

Similar to hypoxia, the dose, pattern, and exposure frequency of hypercapnia influences the physiological adaptations that occur following exposure. Since hypercapnia seldom occurs without the presence of hypoxia, limited studies have evaluated the physiological adaptations to normoxic hypercapnia. Furthermore, to the best of the researcher's knowledge, only one study has been done to determine the effect of intermittent hypercapnia (IHc) on the ventilatory and cardiovascular systems. When exposing participants to 40 minutes of IHc at rest (40 second hypercapnic exposures ($P_{ET}CO_2$ + 5mmHg, O_2 clamped at baseline levels), followed by 20 seconds of normoxic normocapnia (O_2 and CO_2 clamped at baseline levels), a decrease in resting $\dot{V}_E$ occurred up to 30-minutes post IHc. However, this was not indicative of ventilatory long term depression (vLTD) as $P_{ET}CO_2$ was depressed below baseline, and $P_{ET}O_2$ remained relatively unaffected throughout the recovery period. Importantly, systolic blood pressure (SBP), DBP, total peripheral resistance (TPR), and MAP were found to be elevated up to 30-minutes following the cessation of IHc. Long-term facilitation of arterial BP following IHc provides evidence of adaptations along the sympathetic pathway which are

not specific to the respiratory feedback loop. Considering these findings, it is speculated that chemoreceptor desensitization may contribute to changes in $\dot{V}_E$ and cardiovascular augmentation following IHc. Based on a comprehensive review of relevant literature, a summary of theoretical pathways in which IHc may promote plastic changes to facilitate $\dot{V}_E$ and autonomic function is provided in Figure 3.

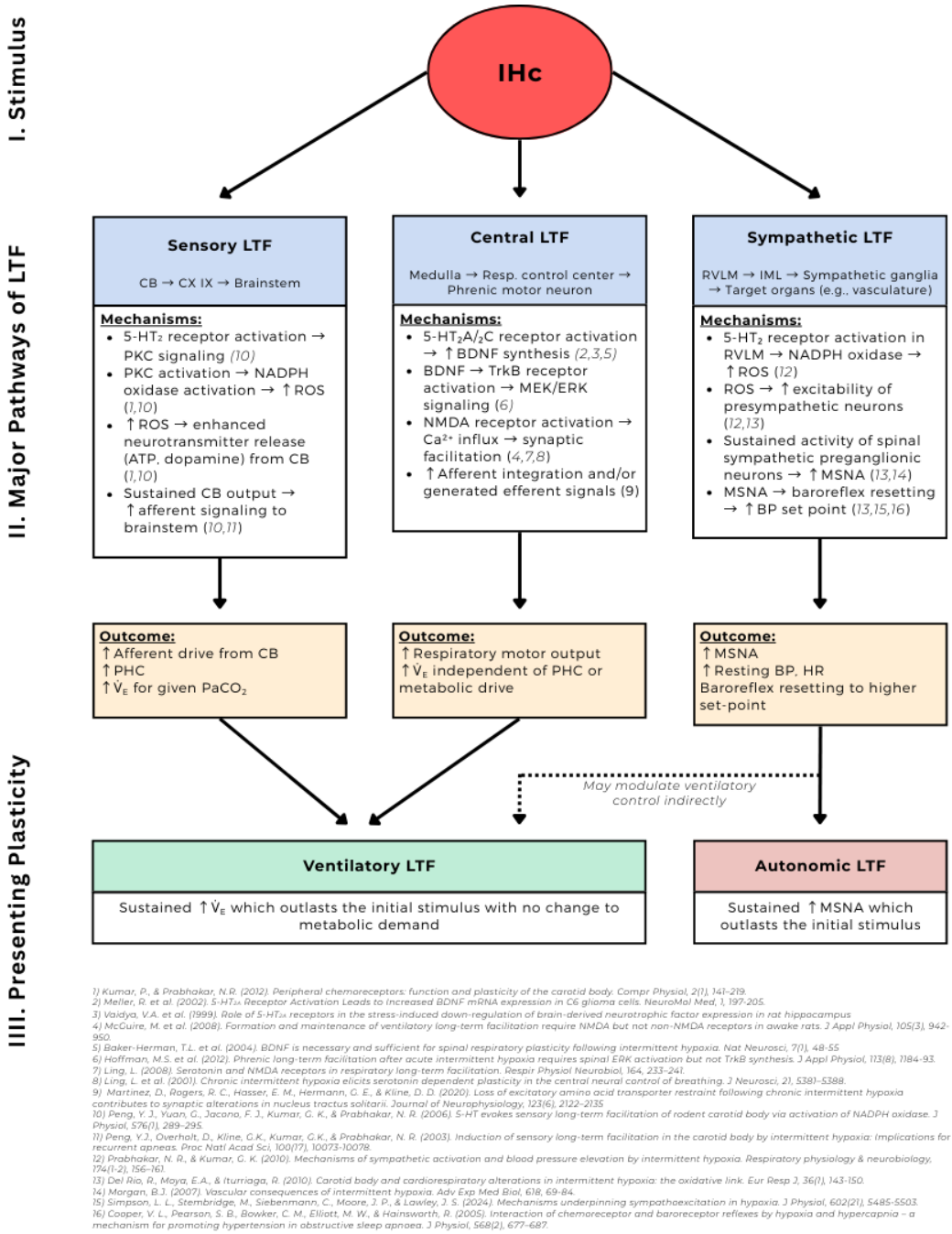


Figure 3. Pathways in which IHc may lead to plastic changes facilitating ventilatory and autonomic function. ATP, adenosine triphsosphate; BNDF, brain-derived neurotrophic factor; CB, carotid body; CO_2, carbon dioxide; CX IX, glossopharyngeal nerve; IHc, intermittent hypercapnic; IML, intermediolateral cell column; LTF, long term facillitation; NADPH, nicotinamide adenine dinucleotide phosphate; NMDA, N-methyl-D-aspartate; NTS, nucleus of the solitary tract; PHC, peripheral hypercapnic chemosensitivity; PKC, protein kinase C; ROS, reactive oxygen species; RVLM, rostral ventrolateral medulla; trkB, tropomyosin receptor kinase B; $\dot{V}_E$, ventilation.

1.7 The Effect of Exercise on the Cardiorespiratory System

Exercise increases cardiorespiratory activity, beginning with feedforward input from the central command system upon the onset of exercise (10). An anticipatory effect has been found such that upon the onset of light exercise, rises in HR and $\dot{V}_E$ occur before changes in metabolic demand or chemoreceptor afferent activity (38,39). Therefore, changes in blood gases are not required to stimulate a cardiorespiratory response with exercise. The pre-emptive increase in cardiorespiratory activity negates a lag period before feedback from peripheral chemoreceptors on arterial pH and CO_2 content can reach the brainstem. As exercise intensity increases, there is a greater metabolic demand for O_2 in the working muscles, as well as a need to expire accumulating metabolic by-product in the blood. With progressive exercise, an initial increase in V_T is observed followed by an elevation in f_B, leading to an overall rise in $\dot{V}_E$ (10). The increase in cardiorespiratory activity with exercise can largely be attributed to increased feedback from chemo- and mechanoreceptors within the body (40).

Exercise increases sympathetic activity to the heart, causing both HR and stroke volume (SV) to rise. SBP follows a nearly linear relationship with exercise intensity due to coinciding increases in $\dot{Q}$, the product of HR and SV. DBP changes minimally due to decreases in TPR required to attain adequate blood distribution (10). The relationship between MAP, $\dot{Q}$, and TPR agrees with Ohm's law of fluid flow where MAP is determined as the product of $\dot{Q}$ and TPR. Given the increase in $\dot{Q}$ overshadows the fall in TPR, MAP increases with progressive exercise.

1.8 The Effect of Exercise on the Respiratory Chemoreflex

A variety of research has evaluated how the respiratory chemoreflex is influenced by exercise. While central chemoreceptors remain unaffected by exercise in healthy individuals due to the stability of CSF pH, peripheral chemoreceptors have been found to increase in sensitivity to CO_2 and O_2 (38,39). Pianosi et al. found the PHC was doubled during steady-state exercise in comparison

to at rest (38). Similarly, a study which evaluated the HVR during exercise and at rest found the response enhanced during exercise (8). These findings suggest that peripheral chemoreceptor activity is increased in an active state.

Chapter 2
Study Rationale

Resting $\dot{V}_E$ is fine-tuned by tonic peripheral chemoreceptor input. IH has been found to increase sympathetic nerve activity (SNA) and sensitize the CB to arterial O_2 and CO_2 challenges through changes in plasticity, thereby leading to a lasting increase $\dot{V}_E$ drive and cardiac function at rest. Spinal synaptic enhancements with IH have been leveraged therapeutically to improve respiratory function in individuals with spinal cord injuries (83). However, while IH is well characterized, the role of IHc remains largely unexplored despite its frequent co-occurance in natural instances of IH, such as in obstructive sleep apnea (OSA). In OSA, IHc accompanies IH, yet its independent contributions to cardiorespiratory control are poorly understood while comorbidities such as systemic hypertension and metabolic dysfunction are attributed solely to chronic IH (84).

The presence and control of CO_2 during IH plays an important role in the manifestation of adaptations. Studies have shown that vLTF only occurs with coinciding IHc, or a sustained elevation in CO_2. Limited research has investigated adaptations following IHc without the presence of hypoxia. A recent study by Shing et al. (2025) found evidence of long-term facilitation of arterial BP following IHc, as resting SBP, DBP, MAP, and TPR remained elevated following exposure, although minimal changes in $\dot{V}_E$ were observed (7). There has been no research to date investigating possible mechanisms underpinning adaptations following IHc. Therefore, one goal of this study is to isolate the effect of cyclic exposures to high levels of CO_2 on PHC as a possible mechanism for changes in cardiorespiratory function. The disentanglement of hypercapnia's unique physiological impacts from IH will help refine our understanding of its role in autonomic dysregulation.

Exercise also increases $\dot{V}_E$ and MAP, in addition to enhancing peripheral chemosensitivity to changes in arterial O_2 and CO_2. Studies that aimed to evaluate the additive effects of exercise and

sustained hypercapnia found enhancements in peripheral and central respiratory chemosensitivity, as well as the augmentation of $\dot{V}_E$ in a manner suggestive of vLTF (9). However, there has been no research to date employing acute cyclic exposures to hypercapnia for the purpose of isolating peripheral chemoreceptor input when observing the cumulative effect of CO_2 and exercise on cardiorespiratory function. This study will therefore employ exercise as an added physiological stimulus to examine its potential modulatory role in mechanisms governing plastic changes following IHc.

Chapter 3
Research Questions and Hypotheses

Research Questions:

1. Will resting MAP at Post, Post-25, and Post-35 be elevated from Pre following IHc in comparison to time-matched control?
2. Will resting $\dot{V}_E$ be depressed Post relative to Pre following IHc in comparison to time-matched control?
3. Will exercising PHC be elevated at Ex-Post from Ex-Pre following IHc in comparison to time matched control?
4. Will resting PHC be elevated at Post from Pre following IHc in comparison to time-matched control?

Hypotheses:

1. Resting MAP will be elevated from Pre at Post, Post-25, and Post-35 following IHc in comparison to time-matched control.
2. Resting $\dot{V}_E$ will be depressed at Post compared to Pre following IHc, whereas resting $\dot{V}_E$ will show no significant differences between Pre and Post with control.
3. Exercising PHC at Ex-Post will be elevated from Ex-Pre with IHc, relative to time-matched control.
4. Resting PHC will be elevated at Post from Pre with IHc, relative to time-matched control.

Chapter 4
Methods

4.1 Ethics

The experimental procedures for this study were approved by the Clinical Research Ethics Board at the University of Waterloo (CREB #45352). The research methods and protocols adhered to the recommendations outlined by the *Declaration of Helsinki* concerning the use of human participants, with the exception of registrations in a database.

4.2 Participants

Twenty young healthy adults (n=10 female) with no known respiratory or cardiovascular conditions were recruited to participate in this study. Table 1 outlines the specific inclusion and exclusion criteria for the participants. Participants were excluded if they had symptoms of cardiovascular, respiratory, or metabolic diseases, or were taking any medications that impact cardiovascular function. All participants were screened for healthy pulmonary function using full body plethysmography according to American Thoracic Society guidelines (41). Participants were included in the study if they demonstrated >80% of their predicted values, for forced vital capacity (FVC), forced expiratory ratio (FEV_1/FVC), peak expiratory flow, total lung capacity (TLC), and diffusion capacity of the lung for carbon monoxide (DLCO).

The proposed sample size was 22 participants (n = 11 female). The sample size calculation was based on previous work that measured ventilatory changes following IHc at rest (85). The study employed a similar crossover design, where a group of 15 participants (5 females) were subjected to both IHc and a placebo. A 1.2 L/min (p=0.052) decrease in $\dot{V}_E$ was observed 30-minutes following IHc exposure. Based on an effect size of 0.6857, the expected sample size required for the current study was n = 19 to detect a 1.2 L/min decrease in $\dot{V}_E$ between the experimental and control group. A

total of n = 22 were recruited to account for participant dropout. The anticipated change in BP was greater than that of $\dot{V}_E$. In the same study, an 8.6mmHg (p=<0.001) increase in MAP was observed 30 minutes following IHc. Therefore, $\dot{V}_E$ was utilized as the endpoint for the determination of sample size in the current study to ensure sufficient power.

Table 1: Participant inclusion and exclusion criteria

Inclusion Criteria	**Exclusion Criteria**
• Age: 18-40 years • Active: 3+ days per week for a total of 150 minutes per week • Normal pulmonary function	• Presence of chronic health condition(s) [i.e. metabolic (i.e. Type 1 or Type 2 diabetes), cardiovascular (i.e. hypertension), gastrointestinal, or respiratory (i.e. chronic pulmonary obstructive disorder)] • Arthritis • Current smoker • Obstructive sleep apnea • Not within normal weight limits, BMI 18.5-30 kg/m^2 • Pregnant, or possibility of pregnancy, or nursing • Taking a progesterone-only birth control • Tested positive for COVID-19 within the last 28 days and have not resumed exercising at the same level prior to the diagnosis • Inability to complete the exercise sessions

4.3 Experimental Overview

All participants completed 3 testing days (Figure 4). The first day consisted of screening, a graded maximal exercise test to determine workload, and familiarization with the End-Tidal Forcing (ETF) system and chemosensitivity testing protocols. The second and third days of the study comprised the experimental protocol. On these days, participants completed submaximal exercise while receiving IHc or a placebo (room air). The order of experimental conditions was randomized, with each participant completing each condition only once. There was a >48-hour washout period between the experimental conditions.

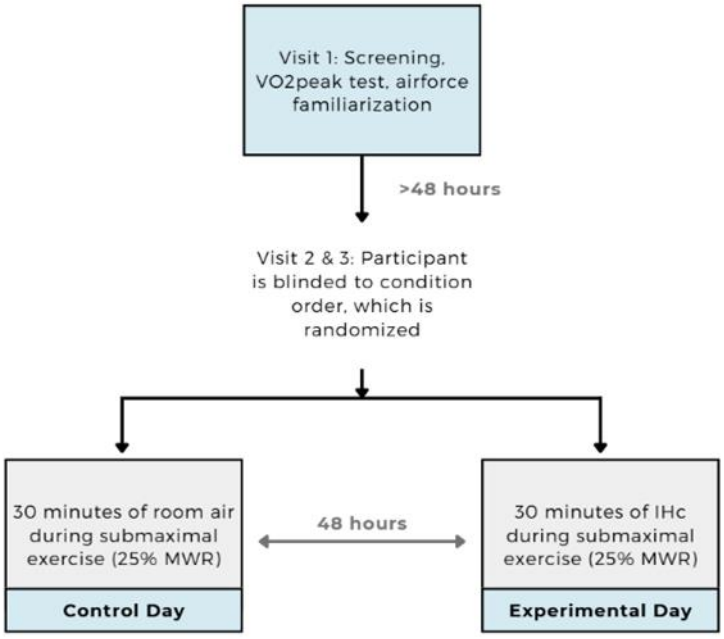


Figure 4. Schematic of overall study protocol. VO_2, oxygen uptake; MWR, maximal work rate (Watts); IHc, intermittent hypercapnia.

4.3.1 Day Day One: Screening, $\dot{V}O_{2max}$ Testing, and Air Force Familiarization

Day one of testing began with participant screening to determine any potential exclusions. Spirometry and lung volumes were assessed using a custom-designed volume-displacement body plethysmography, and performed according to published standards (41) to determine eligibility. The participant was then instrumented for continuous measurements of HR and SpO_2 via a 3-lead ECG (ePM 12M; Mindray North America, Mahway, New Jersey) and finger pulse oximeter (model 7500FO, Nonin, Plymouth, MN, USA), respectively. Participants were fitted with a mask connected to a three-way valve with expired gases collected in a 5L mixing chamber via large bore tubing. A sample line was connected to the port on the facemask to collect end-tidal O_2 and CO_2 (AEI Technologies S-3-A/I, Applied Electrochemistry, Bastrop, TX). Mixed expired O_2 and CO_2 concentrations were continuously collected from a sample line from the mixing chamber (AEI Technologies CD-3Am, Applied Electrochemistry, Bastrop, TX) while inspired and expired flows

were collected from pneumotachometers (model 3813; Hans Rudolph) with the expired pneumotachometer heated to 37°C, allowing for the calculation of the individuals maximal O_2 consumption ($\dot{V}O_{2max}$) during exercise in STPD. Ventilation is expressed in body temperature pressure saturated (BTPS).

Baseline measurements were collected during a 5-minute rest period on a recumbent cycle ergometer (929900; Lode B.V. Medical Technologies, Groningen, Netherlands). The participant then completed a 5-minute warm-up at a self-selected intensity, followed by a brief period of rest. On the participant's mark, the ramp incremental exercise protocol began. Males began at 60 watts (W) and females at 40W, with work rate increasing 20W per minute. The testing protocol was terminated once participants reached volitional fatigue(42). A respiratory exchange ratio (RER) above 1.05 was a secondary endpoint. The participant then completed a 5-minute self-selected cooldown.

Following the cooldown period, the inspired side of the breathing circuit was transferred to the ETF system. A pneumotachograph was placed between the facemask and the 3-way valve for the collection of dual flow measurements. The participants continued to rest while breathing room air through the ETF system for 5 minutes. This was followed by a familiarization with the PHC testing protocol, described in the PHC testing subsection (4.3.3).

4.3.2 Day 2 and 3: Experimental Protocol

Days two and three comprised the experimental portion of the study, whereby the subjects completed submaximal exercise while being exposed to IHc or room air, followed by an observational period. Both days followed the same protocol, apart from whether the participant was administered IHc or room air. All subjects completed both conditions in a randomized order, separated by 48 hours. Participants were blinded to the condition.

Upon reporting to the lab, the participant was instrumented for continuous measurements of HR, SpO_2, $\dot{V}_E$, $P_{ET}CO_2$, $P_{ET}O_2$, and V_T in the same manner as on day 1, with the addition of a rebreathing system (Figure 7). SBP, DBP, and MAP were measured by both a finger (Human NIBP Nano Interface; ADInstruments, Colorado Springs, CO, USA) and brachial (ePM 12M; Mindray North America, Mahway, New Jersey) BP cuff. Following instrumentation, the participant rested on the recumbent cycle ergometer for 5 minutes, followed by a round of PHC testing. The participant then began recumbent cycling at 25% of their maximal work rate (MWR), as determined by the $\dot{V}O_{2max}$ test completed during the first day of testing. Following 5 minutes of cycling, a round of PHC testing was completed while the workload was maintained.

The participant maintained the 25% MWR workload for the next 30 minutes while receiving either IHc or room air. The IHc protocol consisted of 30 cycles of 20s of room air followed by 40s of hypercapnic air (where $P_{ET}CO_2$ was clamped +5mmHg above baseline, and $P_{ET}O_2$ was clamped at normocapnic levels), as depicted in Figure 5**.** During the control day, participants breathed room air for 30 minutes. The ETF system was still running on the control day (due to the noise) for condition-blinding purposes, although it was not attached to the participant's breathing circuit.

Following the final cycle of IHc (or after 30 minutes of placebo), the participants were disconnected from the ETF system while they continued to bike at 25% MWR for 5 minutes in room air. A round of PHC testing was conducted during cycling, and then the participant was instructed to rest with their feet flat on the floor. The PHC testing was conducted once more after 5 minutes of rest. At this point, the facemask was removed, and the participants maintained their position for a 35-minute observational during which BP was continuously monitored. An overview of the experimental protocol and PHC testing time-points can be observed in Figure 6.



Figure 5. An example snippet of raw data for a participant during IHc, which shows the patterning of cyclic $P_{ET}CO_2$ elevations (in red: 40s of +5mmHg; in green: 20s of target baseline values) and clamping of $P_{ET}O_2$ at 100mmHg throughout.

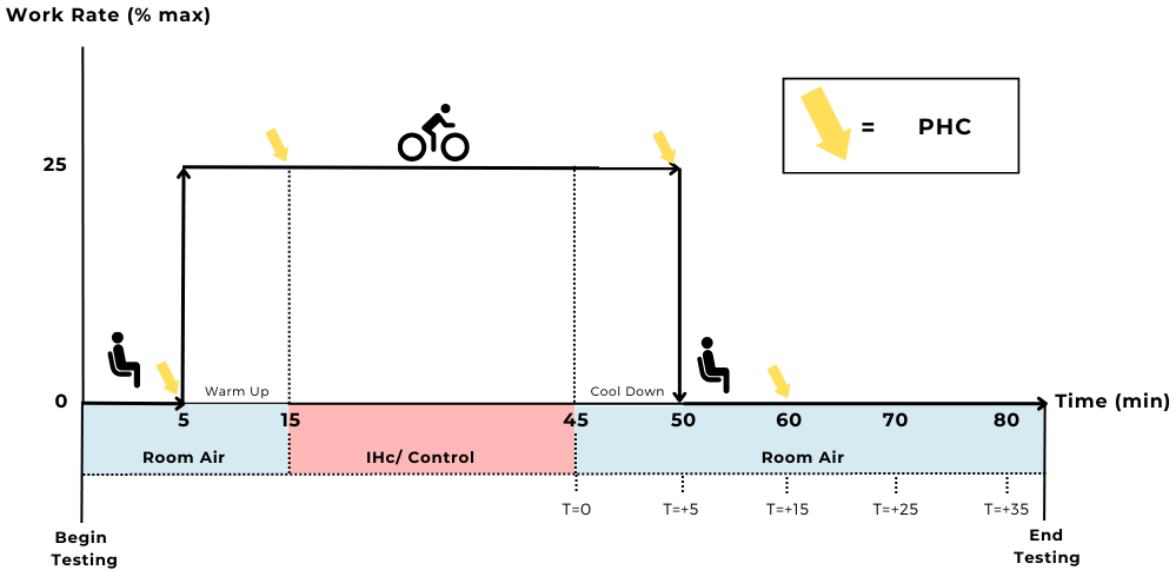


Figure 6. Day 2 and 3 protocol overview. IHc, intermittent hypercapnia (30 x 1 minute cycles of 40s of $P_{ET}CO_2$ +5 mmHg and normoxia: 20s of normoxic normocapnia); $P_{ET}CO_2$, partial pressure of end-tidal carbon dioxide; PHC, peripheral hypercapnic chemosensitivity; T, time since end of condition (minutes).

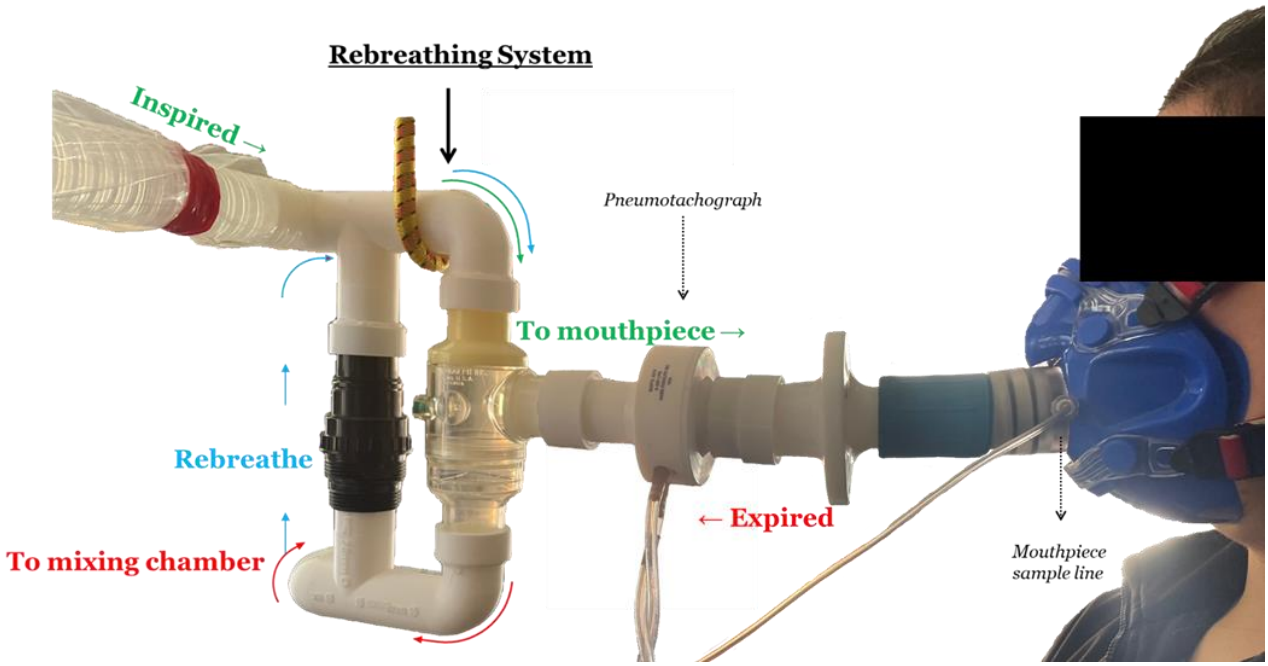


Figure 7. Schematic of the rebreathing system used during days 2 and 3 of testing.

4.3.3 PHC Testing

Each PHC test occurred following a period of room-air breathing to ensure a true baseline and to collect pre-stimulus values for each participant. The hypercapnic gas was made using custom software ('Gas Mixer', Pneumologix), which is interfaced with valves and a control box to allow for accurate gas concentrations. Gas concentrations were verified using O_2 and CO_2 analyzers prior to administration. The gas storage bag was periodically 'fluffed' during testing to prevent gases from settling.

To test the peripheral response to CO_2, two breaths of a hypercapnic gas mixture (10% CO_2, ~20.93% O_2, balance N_2) were administered followed by roughly 45s of room air to allow $P_{ET}CO_2$ and $\dot{V}_I$ to return to pre-stimulus levels. This process was repeated a total of three times per testing cycle. The two breaths were administered to account for the length of tubing between the participants mouthpiece and the Douglas bag of hypercapnic gas. Breaths were administered using a 3-way valve

which was switched between room air and the hypercapnic gas mixture. The timing of the breaths was marked using a handheld piezoelectric pressure sensor interfaced with the data collection system. Neither the marking system nor the valve system were visible or audible to participants, thereby minimizing any anticipatory effects of hypercapnic gas administration (43).

4.4 Data Collection

4.4.1 Cardiorespiratory Measurements

Raw data were recorded at 200 Hz with a 16-channel analog-to-digital data acquisition system (PowerLab/16SP model ML 795; ADInstruments, Colorado Springs, CO). Inspiratory and expiratory flow were continuously measured via pneumotachometers (model 3813; Hans Rudolph). During $VO_{2\,max}$ testing, two pneumotach's were used for individual collection of inspired and expired flows at the beginning and end of the breathing circuit, with expired pneumotachometer heated to 37°C. For the remainder of the study, one heated pneumotach was used between the facemask and three-way valve for the collection of dual flow. The pneumotach was calibrated using room air and a 3L syringe. Calibrated O_2 and CO_2 analyzers (AEI Technologies S-3-A/I and CD-3Am; Applied Electrochemistry, Bastrop, TX) were used to sample mixed-expired gases and end-tidal gases. Mixed-expired gases were sampled from a mixing chamber to allow for the calculation of $\dot{V}O_2$ and $\dot{V}CO_2$. End-tidal gases were sampled at the mouth using a sample line to estimate arterial O_2 and CO_2 tensions, P_aO_2, and P_aCO_2. All collected gases were dried using a nafion tubing inside a sealed glass jar filled with Drierite to ensure the gases contained 0% humidity prior to entering the gas analyzers.

HR was continuously measured using a 3-lead ECG (ePM 12M; Mindray North America, Mahway, New Jersey). BP was measured beat-to-beat using a finometer (Human NIBP Nano Interface; ADInstruments, Colorado Springs, CO, USA) with automatic calibration settings. Two finger cuffs were used, one on each of the second and fourth digits of the left hand, with

measurements switching between the cuffs in 15-minute intervals. Cuff sizes varied based on the participant's finger size, with three cuff sizes available (small, medium, large). Participants were fitted for proper cuff size prior to testing. A height correction unit was used to account for postural BP changes. A brachial BP cuff (ePM 12M; Mindray North America, Mahway, New Jersey) was worn on the right arm, programmed for automated one-time measurements of SBP, DBP, and MAP in 5-minute cycles. Although brachial blood pressure BP measurements were initially collected to correct for potential drift in finometer recordings, inconsistencies in device performance and alignment between methods led to the exclusion of brachial data from final analyses. All reported BP data reflect continuous finometer-derived values. Both participant's arms were supported by wooden arm rests, such that they rested at the participant's side with the elbows bent at approximately 90° and the hands relaxed as seen in figure 8**.**



Figure 8. Experimental instrumentation and set up for cardiovascular measurements. BP, blood pressure; NIBP, non-invasive BP; ECG, electrocardiogram; RA, right arm; LA, left arm; LL, left leg. RA and LA electrodes were placed below the right and left clavicle, respectively, and LL was placed below left lower edge of the rib cage.

4.4.2 Dynamic End-Tidal Forcing

$P_{ET}O_2$ and $P_{ET}CO_2$ were controlled using dynamic ETF during familiarization on day 1, and the 30-minutes of IHc or control on days 2 and 3 (although ETF was not attached to the inspiratory circuit on the control day). This system enabled rapid manipulation of inspired O_2, CO_2, and N_2, achieved through the respective gases being controlled by solenoid valves, thereby enabling the desired gas concentrations to be delivered to a mixing and humidification chamber prior to entering the breathing circuit. Feedback control was achieved through integral and proportional error using purpose-designed software (Labview 13.0, National Instruments, Austin, TX). The system incorporated $P_{ET}O_2$, $P_{ET}CO_2$, inspired, and expired V_T values to maintain desired $P_{ET}O_2$ and $P_{ET}CO_2$ values. The alveolar gas equation was used to estimate CO_2 production and metabolic O_2 consumption to determine the fraction of inspired O_2 (F_IO_2) and CO_2 (F_ICO_2) required to maintain desired $P_{ET}O_2$ and $P_{ET}CO_2$ levels as a feedforward mechanism. The system has been previously used to effectively and rapidly manipulate inspired gas concentrations in an interval fashion, similar to the protocol used in the current study (1,7,44). Similarly, the system has been previously demonstrated as an effective mechanism to control end-tidal gases in the presence of added physiological stressors (45).

4.5 Data Analysis

4.5.1 Cardiorespiratory Parameters

Inspired flow measurements from the pneumotach were numerically integrated to determine volume, from which breathing frequency (f_B) and V_T was derived. Ventilation was calculated as the product of f_B and V_T and is expressed in BTPS. Oxygen consumption was calculated as the difference between inspired and expired O_2 concentration. Oxygen uptake and $\dot{V}CO_2$ were measured when the participant was breathing room air, and are expressed in standard pressure temperature dry (STPD).

HR is calculated as the rate of R-waves recorded by the HR monitor. The finometer provided a continuous finger pressure waveform, sampled at 200 samples/second, of which SBP, DBP, and MAP signals were derived on a beat-to-beat basis. All cardiovascular variables were extracted and analyzed offline on a beat-by-beat basis. One-time SBP, DBP, and MAP measurements were taken via the brachial cuff every 5 minutes.

All ventilatory and cardiovascular measurements were time-aligned and averaged over specific time intervals. Pre and post IHc/control cardiovascular and ventilatory measurements were averaged in 30 second intervals over the final 3 minutes of the overall 5 minute timeframe to ensure steady-state values were captured. For finometer BP measurements at the Post-25 and Post-35 marks, the 30 second intervals were averaged over the entire 5 minute period.

4.5.2 Maximal Exercise Capacity

The work rate achieved at the time of volitional fatigue was recorded as MWR. Volume of O_2 uptake was averaged over the final 20 seconds of the test to determine absolute max O_2 uptake ($\dot{V}O_{2max}$). Relative $\dot{V}O_{2max}$ was determined by dividing absolute $\dot{V}O_{2max}$ by using the participant's body mass (kg), and converting this value to ml/kg/min.

4.5.3 PHC Testing

Pre-stimulus $\dot{V}_I$ and $P_{ET}CO_2$ was averaged over 20 seconds immediately prior to the administration of a stimulus. Peak $\dot{V}_I$ was determined visually as the greatest single breath within 30 seconds of hypercapnic stimuli. Peak $P_{ET}CO_2$ was visually determined as the greatest pressure of CO_2 at the end of an expiration. The change in ventilation and $P_{ET}CO_2$ was determined as the difference between the peak and corresponding pre-stimulus average $\dot{V}_I$ and $P_{ET}CO_2$ (46). The PHC response was determined as the quotient of delta $\dot{V}_I$ by delta $P_{ET}CO_2$ for each hypercapnic round (46). Figure 9 displays an example of one round of PHC testing for a single participant. The response from the three

rounds of transient hypercapnia during each testing cycle was averaged to yield a single overall response at each chemosensitivity testing time point throughout the protocol.

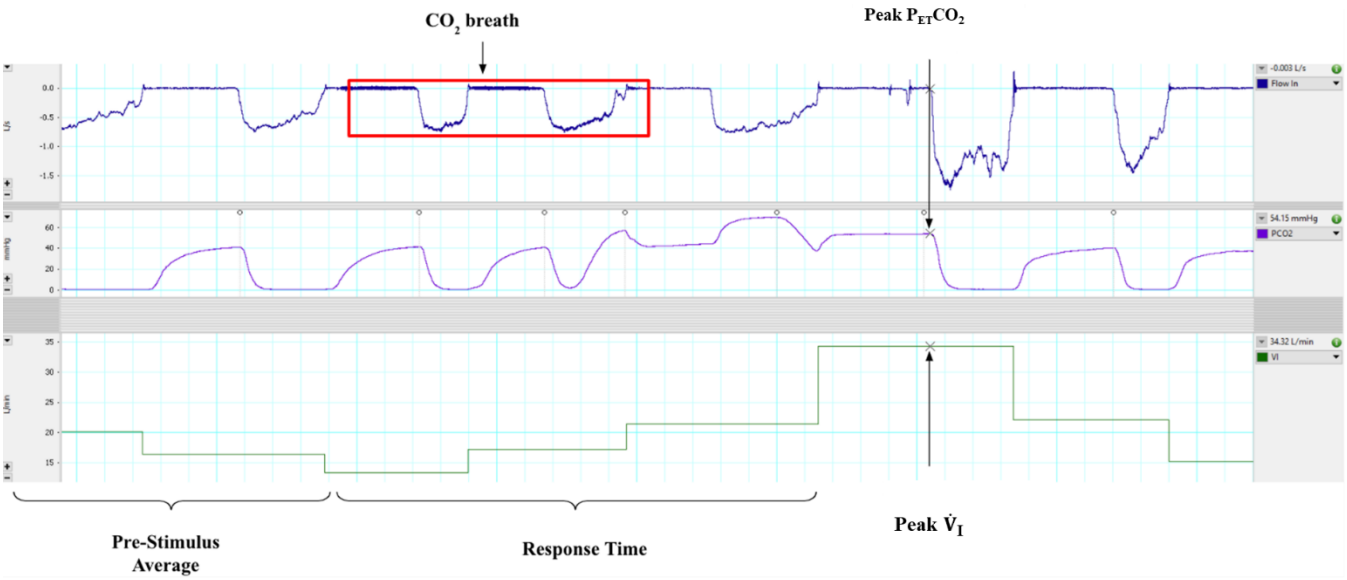


Figure 9. Data acquisitions software (LabChart) showing an example of time-based averages and peak values captured during PHC testing for one participant. CO_2, carbon dioxide; $P_{ET}CO_2$, partial pressure of end-tidal carbon dioxide; $\dot{V}_I$, minute ventilation (inspired).

4.6 Statistical Analysis

Data were analyzed using RStudio (version 3.4.0) using the R-programming language and SigmaPlot (47). A significance level of $p<0.05$ was used, and all tests were two-sided. Paired comparisons were made within subjects between all pre and post condition resting and exercising measurements (within condition) to evaluate the effect of IHc, exercise, and time. Continuously measured variables (HR, $\dot{V}O_2$, $\dot{V}CO_2$, $P_{ET}O_2$, $P_{ET}CO_2$, mixed O_2 and CO_2, $\dot{V}_I$, $\dot{V}_E$, f_B, V_T, finometer SBP, DBP, and MAP) were averaged over 30 second intervals during room air breathing. All resting measurements (Pre, Post, Post-25, Post-35) were grouped into 5-minute bins, with only BP variables measured at Post-25 and Post-35. Measurements during exercise were grouped into 3-minute bins to ensure steady-state was captured. To be distinguishable from resting measurements, all exercising

values are reported as Ex-[Time]. For example, Ex-Post describes a measurement recorded during exercise, post-condition.

An example of raw data for a single participant during both the IHc and control day is displayed in Figure 10. Also highlighted in Figure 10 is the important time-markings and events in which comparisons were made across conditions. Green stars mark the 5-minute averages during rest in room air (Pre, Post, Post-25, Post-35), while blue stars mark the 3-minute averages during exercise in room air (Ex-Pre, Ex-Post). Resting and exercising PHC testing timepoints are marked with pink and orange stars, respectively. Yellow stars mark comparisons made during IHc/control between the first and last 5-minutes of condition.

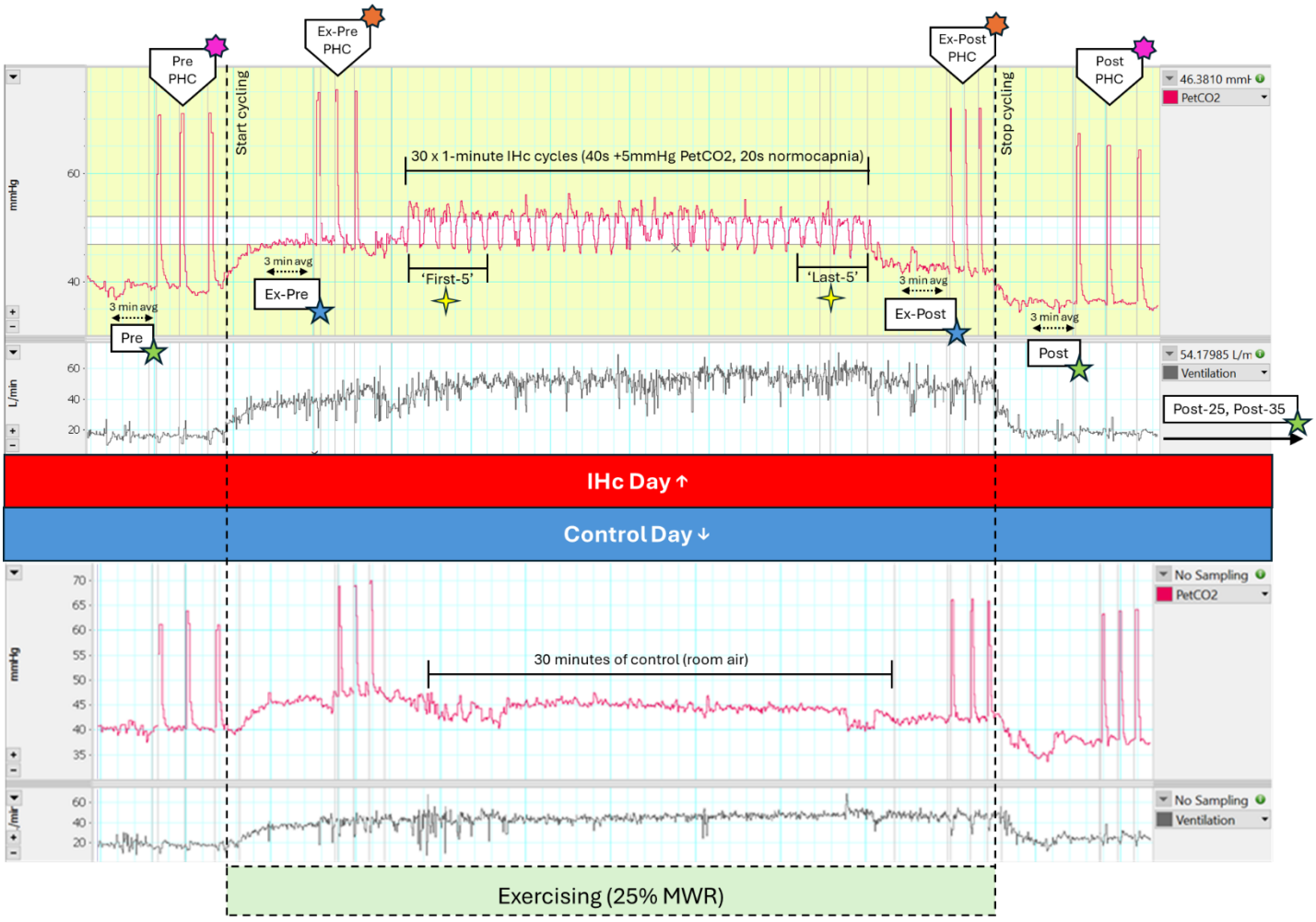


Figure 10. An example of one participant's raw data across both the IHc (top) and control (bottom) days, with additional markings to highlight important time groupings and events where comparisons were made during analysis.

4.6.1 Cardiorespiratory Function

To evaluate the effect of condition (IHc, Control) over time, two-way RM ANOVAs were conducted on all continuously measured variables that met normality assumptions. Bonferroni-corrected Student's t-tests were performed for post-hoc analysis when significant F ratios were detected. For BP variables (brachial and finometer SBP, DBP, and MAP), the factor Time had four levels: Pre, Post, Post-25, and Post-35 marks. For all other variables, Time had two levels: Pre and Post. For measurements recorded during exercise, the levels of time are referred to as Ex-Pre and Ex-Post. Normality and homogeneity of variance were assessed using Shapiro-Wilk and Levene's tests, respectively. ANOVAs were conducted only for variables that satisfied parametric assumptions. Secondary analysis of Δ% from Pre to Post was calculated within participants and averaged across condition.

Variables that did not meet normality or homogeneity assumptions were analyzed using non-parametric methods. The Friedman test was applied to evaluate differences between time and condition pairings. Post-hoc analyses for significant non-parametric findings were conducted using Wilcoxon Signed-Rank tests.

4.6.2 PHC Statistical Analysis

Resting and exercising PHC were analyzed using paired t-tests to compare pre versus post IHc or time-matched control. Delta $P_{ET}CO_2$ and delta $\dot{V}_I$ were used as the coefficient of variation for the chemoresponse and was determined as the quotient of the standard deviation and mean for each participant during each testing stage. Normality and homogeneity of variance were assessed using Shapiro-Wilk and Levene's tests, respectively. Data pairings deemed non-normal were analyzed using the Friedman test, and a Wilcoxon signed-rank test was used for post-hoc analysis. For normally distributed variables, a repeated measures ANOVA (2x2) was used to determine the effect

of IHc on the PHC during exercise with the factors time (Pre, Post) and condition (IHc, control). Similarly, a repeated measures ANOVA (2x2) was used to determine the effect of IHc on the PHC at rest with the factors time (Pre, Post) and condition (IHc, control). Bonferroni-corrected Student's t-tests were performed for post-hoc analysis following significant ANOVA results.

Chapter 5

Results

5.1 Participant Demographics, Baseline Values & Maximal Exercise Testing

Table 2 summarizes descriptive characteristics of 20 participants (10F) and maximal exercise testing results from Day 1. A significant difference was observed between males and females in height, MWR, absolute and relative $\dot{V}O_{2max}$.

Table 2. Participant demographics and maximal exercise test results.

	Full Group (n=20)	***Females (n=10)***	***Males (n=10)***	***p- value***
Age (yrs)	*24 ± 4*	*24 ± 3*	*25 ± 5*	*0.644*
Height (cm)	*172 ± 7*	*167 ± 7*	*176 ± 4**	*0.015*
Body Mass (kg)	*72 ± 11*	*68 ± 11*	*76 ± 10*	*0.072*
BMI (kg/m^2)	*25 ± 3*	*24 ± 3*	*25 ± 3*	*0.924*
MWR (Watts)	*242 ± 50*	*208 ± 43*	*276 ± 30**	*0.004*
Absolute $\dot{V}O_{2max}$ (L/min)	*2.7 ± 0.7*	*2.3 ± 0.5*	*3.2 ± 0.6**	*0.003*
Relative $\dot{V}O_{2max}$ (mL/kg/min)	*37.8 ± 8.0*	*33.6 ± 5.9*	*41.9 ± 7.9**	*0.004*
$\dot{V}_E$ (L/min)	*115 ± 28*	*95 ± 20*	*134 ± 22**	*<0.001*
HR (bpm)	*178 ± 10*	*177 ± 8*	*179 ± 12*	*0.653*
RER	*1.20 ± 0.04*	*1.19 ± 0.04*	*1.20 ± 0.04*	*0.712*

*Values are mean ± SD. BMI, body-mass index; MWR, maximal work rate; $\dot{V}O_{2max}$, volume of oxygen consumption averaged over the last 20s of graded-maximal exercise test; $\dot{V}_E$, ventilation at maximal exercise; HR, heart rate at maximal exercise; RER, respiratory exchange ratio at maximal exercise. *Significantly different from females ($p<0.05$).*

Table 3 reports baseline measurements between control and IHc days. There were no significant differences in any variables at rest or during exercise between the two experimental days. No comparisons were made between rest and exercise within or between days.

Table 3. Baseline resting and exercising measurements between conditions.

Baseline Values

	Rest			**Exercise**		
	Control	*IHc*	*p- value*	*Control*	*IHc*	*p- value*
V_T (L)	1.07 ± 0.3	1.12 ± 0.4	0.440	1.73 ± 0.4	1.67 ± 0.4	0.489
f_B (breaths/min)	15.0 ± 4.4	14.6 ± 4.9	0.586	21.3 ± 4.1	21.1 ± 3.7	0.790
$\dot{V}_E$ (L/min)	15.8 ± 3.1	14.5 ± 2.7	0.073	35.3 ± 6.5	33.9 ± 6.6	0.462
$P_{ET}O_2$ (mmHg)	104 ± 4.1	104 ± 5.2	0.824	103 ± 4.3	102 ± 4.6	0.587
$P_{ET}CO_2$ (mmHg)	40.5 ± 3.4	40.2 ± 3.7	0.751	44.3 ± 4.5	44.3 ± 3.9	0.915
$\dot{V}O_2$ (L/min)	0.32 ± 0.08	0.29 ± 0.07	0.171	1.09 ± 0.21	1.05 ± 0.22	0.416
$\dot{V}CO_2$ (L/min)	0.27 ± 0.08	0.24 ± 0.07	0.464	0.89 ± 0.19	0.86 ± 0.24	0.688
HR (bpm)	75 ± 11	72 ± 12	0.353	103 ± 12	102 ± 11	0.823
SBP (mmHg)	128 ± 17	128 ± 17	0.947	156 ± 15	162 ± 17	0.321
DBP (mmHg)	74 ± 13	74 ± 13	0.972	74 ± 12	81 ± 12	0.110
MAP (mmHg)	89 ± 14	92 ± 14	0.625	99 ± 12	106 ± 12	0.087

Values are mean ± SD. V_T, tidal volume; f_B, frequency of breathing; $\dot{V}_E$, ventilation; $P_{ET}O_2$, partial pressure of end-tidal oxygen; $P_{ET}CO_2$, partial pressure of end-tidal carbon dioxide; $\dot{V}O_2$, volume of oxygen consumption; $\dot{V}CO_2$, volume of carbon dioxide consumption; HR, heart rate; SBP, systolic blood pressure; DBP, diastolic blood pressure, MAP, mean arterial pressure.

5.2 Cardiovascular Responses at Rest

A summary of resting cardiovascular responses can be found in table 4. It should be noted that brachial BP measurements are excluded from the results. All reported BP values reflect finometer measurements, for reasons specified in *Section 4.4.1. Cardiorespiratory Measurements*. A significant interaction effect of condition x time was observed in resting HR ($p = 0.004$). Post hoc analysis using

a Bonferroni-corrected Student's t-tests for multiple pairwise comparisons highlighted significant increases in HR from Pre to Post with both conditions, although this difference was more than two-fold greater with IHc (IHc: Δ16.3bpm, $p < 0.001$; control: Δ7.7bpm, $p = 0.004$).

Of all BP metrics, which were observed over an additional two time points at rest (Post-25, Post-35), DBP was the only variable to show a significant effect, highlighted as a main effect of time ($p = 0.03$). Post-hoc analysis revealed a significant elevation in DBP at Post-25 from Pre across both conditions (Post-25: +4.4mmHg, $p = 0.050$). Resting HR and BP outcomes are visualized across time and conditions in Figure 11.

Table 4. Average resting cardiovascular responses across time and conditions.

	REST										
	Control				IHc				*p-values*		
	Pre	*Post*	*Post-25*	*Post-35*	*Pre*	*Post*	*Post-25*	*Post-35*	*Interaction*	*Condition*	*Time*
HR, bpm	*75 ± 11*	*83 ± 14**	-	-	*72 ± 12*	*88 ± 14**	-	-	***0.004***	*0.739*	*<0.001*
SBP, mmHg	*128 ± 17*	*129 ± 19*	*131 ± 18*	*131 ± 15*	*128 ± 17*	*125 ± 16*	*133 ± 15*	*130 ± 13*	*0.585*	*0.768*	*0.117*
DBP, mmHg	*74 ± 13*	*77 ± 12*	*77 ± 14**	*77 ± 11*	*74 ± 13*	*75 ± 10*	*80 ± 14**	*79 ± 11*	*0.283*	*0.720*	***0.030***
MAP, mmHg	*89 ± 14*	*93 ± 13*	*93 ± 14*	*93 ± 12*	*92 ± 14*	*91 ± 10*	*97 ± 14*	*95 ± 12*	*0.317*	*0.566*	*0.058*

*Values are mean ± SD. IHc, intermittent hypercapnia; HR, heart rate; SBP, systolic blood pressure; DBP, diastolic blood pressure; MAP, mean arterial pressure. * Significant effect of time ($p < 0.05$).*

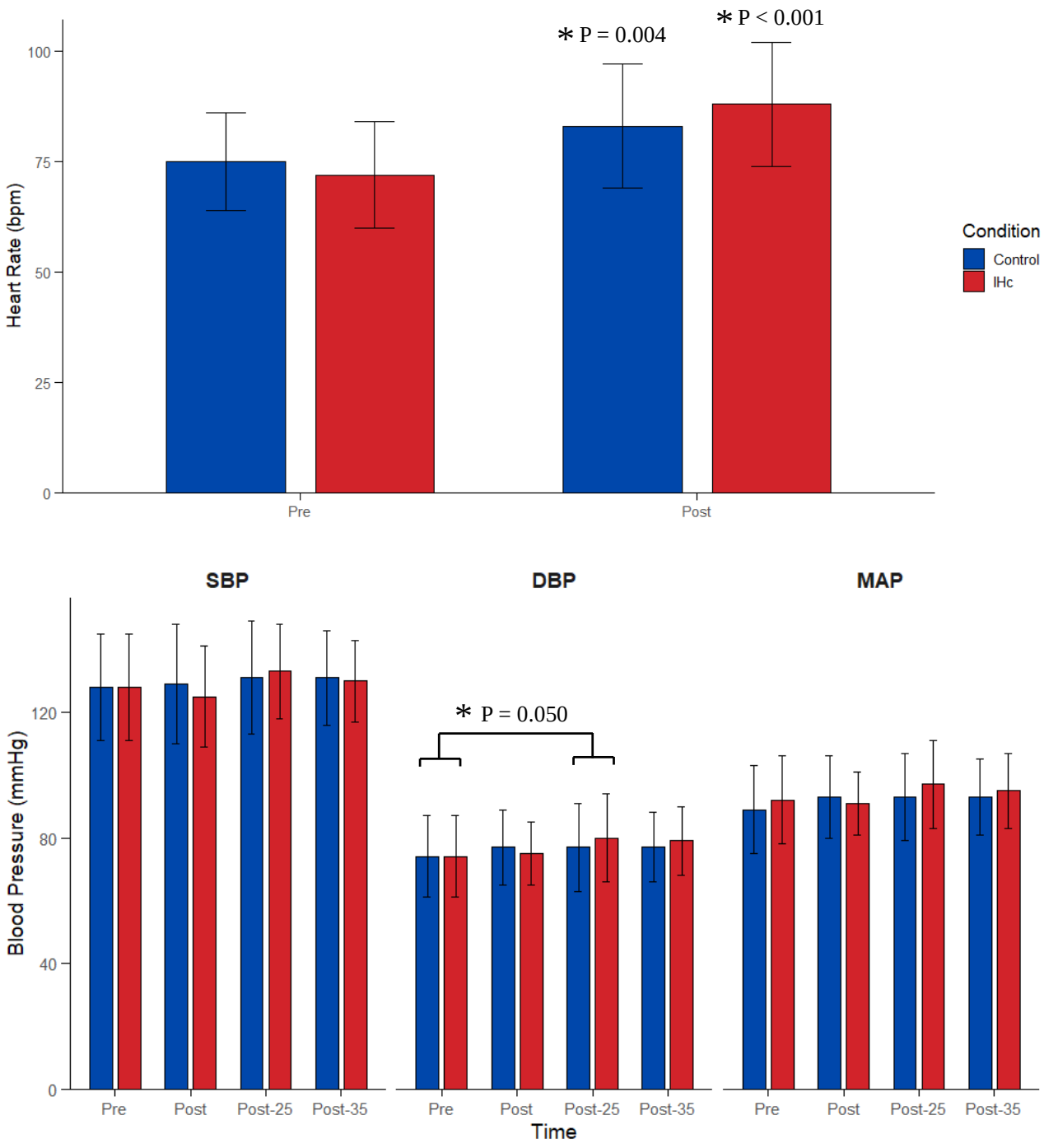


Figure 11. Average ± SD resting HR and BP across time and conditions. Significant time effects showed Post HR was elevated from Pre within conditions IHc (+16.3bpm, $p < 0.001$) and control (+7.7bpm, $p = 0.004$). DBP at Post-25 was elevated from Pre across both conditions (+4.4mmHg, $p = 0.050$). IHc, intermittent hypercapnia; HR, heart rate; SBP, systolic blood pressure; DBP, diastolic blood pressure; MAP, mean arterial pressure. * Significantly different from Pre ($p< 0.05$).

5.3 Cardiovascular Responses during Exercise

A summary of exercising cardiovascular responses is presented in table 5. A Friedman RM ANOVA on ranks revealed significant differences in exercising HR between the different combinations of condition and time ($p < 0.001$). Notably, post hoc analysis highlighted a significant increase from Ex-Pre to Ex-Post with IHc (Δ11.8bpm, $p < 0.001$) which was non-significant with time-matched control (Δ6.1bpm, $p = 0.203$). Exercising HR was also significantly different between IHc Ex-Post and control Ex-Pre ($p = 0.025$), and between IHc Ex-Pre and control Ex-Post ($p = 0.005$). Significant differences were also observed in exercising MAP across time and condition pairings ($p = 0.001$). Post-hoc analysis revealed a significant decrease in exercising MAP from Ex-Pre to Ex-Post with IHc (Δ8.1mmHg, $p = 0.006$) which was non-significant with time-matched control (Δ5.2mmHg, $p = 0.072$)

A two-way RM ANOVA highlighted a main effect of time in exercising SBP ($p = 0.002$). Post-hoc analysis revealed significant decreases from Ex-Pre to Ex-Post across both conditions (Δ11.4mmHg, $p = 0.002$). A condition effect was observed for DBP during exercise ($p=0.043$), which was elevated by 4.7± 2.2mmHg across both IHc time points in comparison to control. Exercising HR and BP outcomes are visualized across time and conditions in Figure 12.

Table 5. Average exercising cardiovascular measurements across time and conditions.

	EXERCISE								
	Control			IHc			*p-values*		
	Ex-Pre	*Ex-Post*	*%Δ*	*Ex-Pre*	*Ex-Post*	*%Δ*	*Interaction*	*Condition*	*Time*
HR, bpm	*103 ± 12*	*109 ± 14*	*6%*	*102 ± 11*	*114 ± 15**	*12%*	***< 0.001 (Friedman)***	*N/A*	*N/A*
SBP, mmHg	*156 ± 15*	*145 ± 19**	*-7%*	*161 ± 17*	*150 ± 23**	*-7%*	*0.969*	*0.143*	***0.002***
DBP, mmHg	*75 ± 12*	*71 ± 11*	*-3%*	*81 ± 12†*	*75 ± 13†*	*-7%*	*0.231*	***0.043***	*0.070*
MAP, mmHg	*99 ± 12*	*94 ± 12*	*-5%*	*106 ± 12*	*98 ± 15**	*-7%*	***0.001 (Friedman)***	*N/A*	*N/A*

*Values are mean ± SD. IHc, intermittent hypercapnia; HR, heart rate; SBP, systolic blood pressure; DBP, diastolic blood pressure; MAP, mean arterial pressure. * Significant effect of time ($p < 0.05$). † Significant effect of condition ($p < 0.05$)*

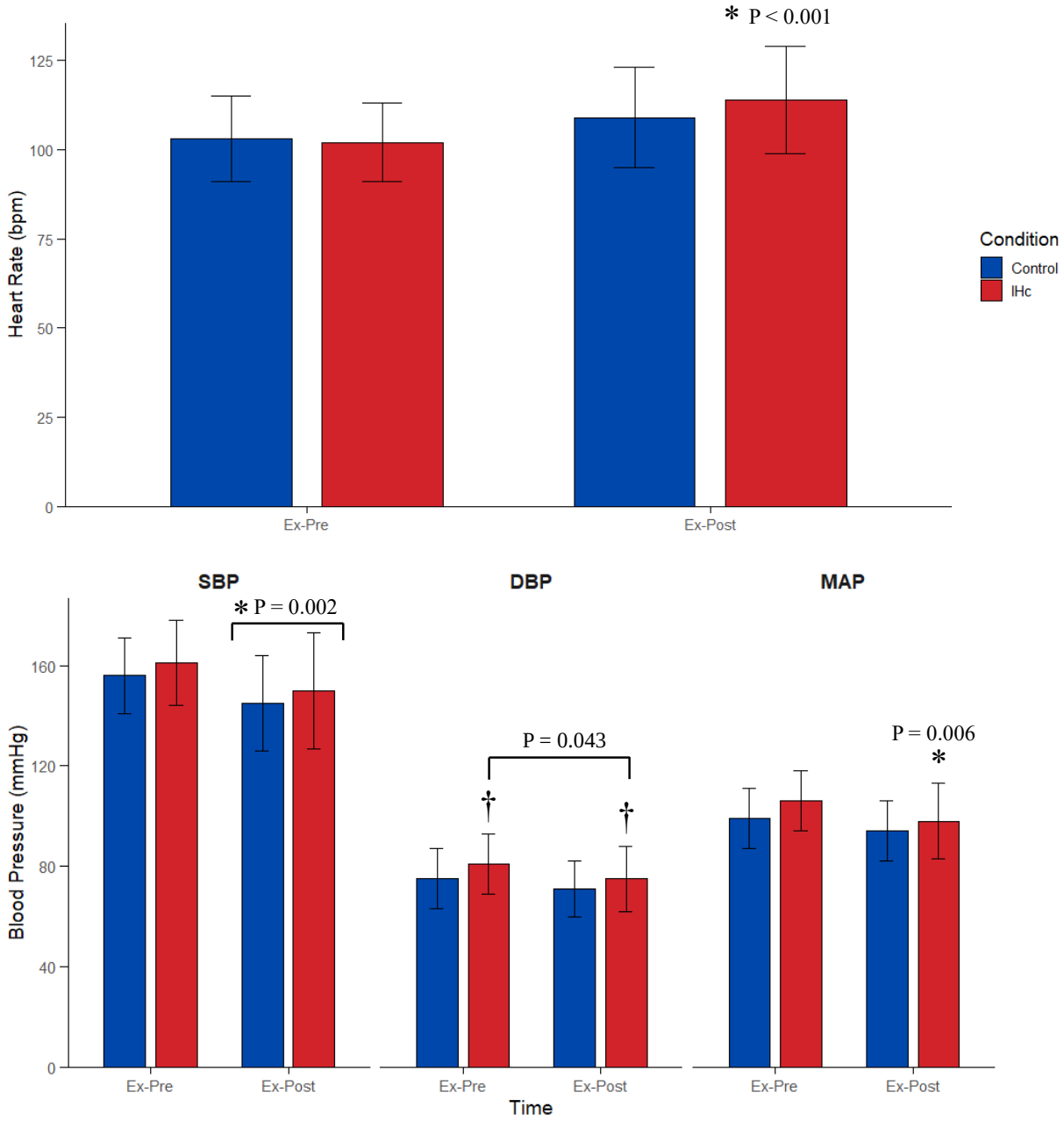


Figure 12. Average ± SD exercising HR and BP across time and conditions. Compared to Ex-Pre, HR at Ex-Post was elevated with IHc (+11.8bpm, $p < 0.001$) but not time-matched control. SBP decreased from Ex-Pre to Ex-Post across both conditions (-11.4mmHg, $p = 0.002$). With IHc, DBP appeared generally elevated across both time points relative to control (IHc: +4.7mmHg, $p = 0.043$). MAP decreased significantly from Ex-Pre to Ex-Post (-8.1mmHg, $p = 0.006$) but not with control. HR, heart rate;.DBP, diastolic blood pressure; MAP, mean arterial pressure, SBP, systolic blood pressure; IHc, intermittent hypercapnia. * Significantly different from Pre ($p < 0.05$). † Significantly different from control ($p < 0.05$).

5.4 The Control of Ventilation at Rest

Table 6 provides a summary of mean resting ventilatory constituents and metabolics across time and conditions. Significant differences were observed in median values of $\dot{V}_E$ across conditions and time ($p < 0.001$). Post-hoc analysis revealed a significant increase in $\dot{V}_E$ from Pre to Post IHc (Δ2.19 L/min, $p < 0.001$), which was not significant in the time-matched control (Δ1.85 L/min, $p = 0.122$)(Figure 13). Meanwhile, a main effect of time was observed in f_B ($p = 0.023$). Post hoc analysis revealed f_B increased significantly from Pre to Post across conditions (+1.7 breaths/min, p= 0.023) Figure 13). Similarly, post-hoc analysis for the main effect of time in $\dot{V}_E / \dot{V}_A$ ($p = 0.002$) revealed an increase from Pre to Post across both conditions (+0.02, $p = 0.002$).

Post-hoc analysis for the main effect of time in $P_{ET}CO_2$ ($p < 0.001$) revealed general decreases from Pre to Post with both conditions (-2.6mmHg, $p < 0.001$). On the other hand, the main effect of time in $P_{ET}O_2$ ($p < 0.001$) highlighted general increases from both Pre to Post with both conditions (+3.1mmHg, $p < 0.001$).

Table 6. Average resting ventilatory activity across time and conditions.

	REST								
	Control			IHc			p-values		
	Pre	*Post*	*%Δ*	*Pre*	*Post*	*%Δ*	*Interaction*	*Condition*	*Time*
$\dot{V}_E$, L/min	*15.8 ± 3.1*	*17.7 ± 3.8*	*13%*	*14.5 ± 2.7*	*16.7 ± 2.2**	*17%*	***<0.001 (Friedman)***	*N/A*	*N/A*
f_B, breaths/min	*15 ± 4*	*18 ± 4**	*18%*	*16 ± 5*	*17 ± 4**	*18%*	*0.710*	*0.792*	***0.023***
V_T, L	*1.1 ± 0.3*	*1.0 ± 0.4*	*-7%*	*1.1 ± 0.4*	*1.1 ± 0.3*	*11%*	*0.061*	*0.644*	*0.305*
$\dot{V}O_2$, L/min	*0.3 ± 0.1*	*0.4 ± 0.1*	*6%*	*0.3 ± 0.1*	*0.3 ± 0.1*	*7%*	*0.621*	*0.556*	*0.108*
$\dot{V}CO_2$, L/min	*0.3 ± 0.1*	*0.3 ± 0.1*	*13%*	*0.2 ± 0.1*	*0.3 ± 0.1*	*16%*	*0.524*	*0.803*	*0.118*
$P_{ET}O_2$, mmHg	*104 ± 4*	*107 ± 5**	*-1%*	*104 ± 5*	*108 ± 3**	*0.4%*	*0.289*	*0.752*	***<0.001***
$P_{ET}CO_2$, mmHg	*41 ± 3*	*38 ± 3**	*0.4%*	*40 ± 4*	*38 ± 3**	*1%*	*0.733*	*0.816*	***<0.001***
$\dot{V}_E$ / $\dot{V}_A$	*1.4 ± 0.5*	*1.4 ± 0.2**	*17%*	*1.5 ± 0.6*	*1.5 ± 0.4*	*8%*	*0.222*	*0.414*	***0.002***

Values are mean ± SD. IHc, intermittent hypercapnia; $\dot{V}_E$, ventilation; f_B, frequency of breathing; V_T, tidal volume; $\dot{V}O_2$, volume of oxygen consumption; $\dot{V}CO_2$, volume of carbon dioxide consumption; $P_{ET}O_2$, partial pressure of end-tidal oxygen; $P_{ET}CO_2$, partial pressure of end-tidal carbon dioxide; $\dot{V}_A$, alveolar ventilation. Significant effect of time ($p < 0.05$).*

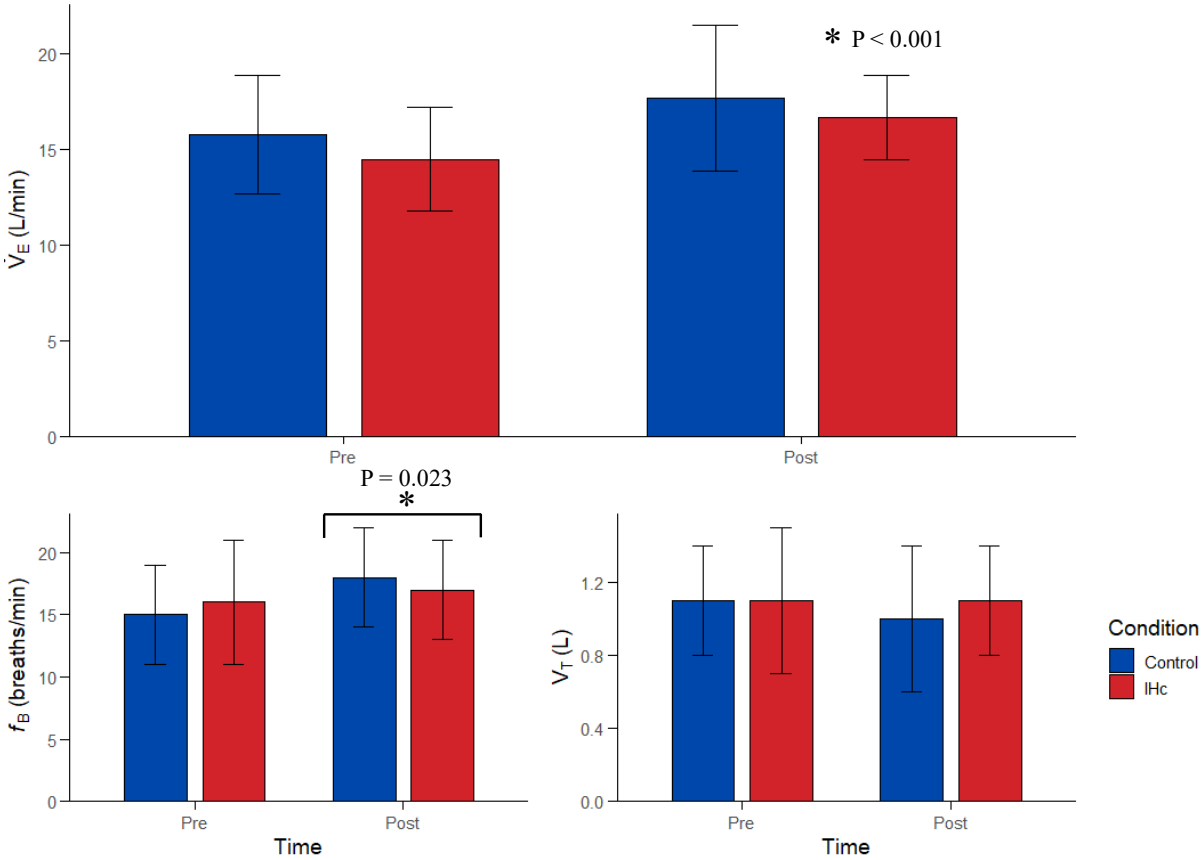


Figure 13. Average ± SD ventilation, breathing frequency, and tidal volume at rest across time and conditions. $\dot{V}_E$ at Post appeared elevated from Pre in the IHc condition (+2.2L/min, $p < 0.001$). f_B was elevated at Post from Pre across both conditions (+1.7 breaths/min, $p = 0.023$). IHc, intermittent hypercapnia; $\dot{V}_E$, ventilation; f_B, frequency of breathing; V_T, tidal volume. * Significantly different from Pre ($p < 0.05$).

5.5 The Control of Ventilation during Exercise

A Friedman RM ANOVA on ranks highlighted significant differences in $\dot{V}_E$ across the different levels of time and condition during exercise ($p < 0.001$). Post hoc analysis revealed that $\dot{V}_E$ increased significantly from Ex-Pre to Ex-Post with IHc (Δ4.9 L/min, $p < 0.001$) but not with control (Δ3.1 L/min, $p = 0.108$)(Figure 14). Similarly, significant differences were observed between the different pairings of condition and time in V_T during exercise ($p < 0.001$). Post hoc analysis revealed

that a significant decrease in exercising V_T from Ex-Pre to Ex-Post with control (Δ0.18L, p = 0.002) was not present with IHc (Δ0.09L, p = 0.159)(Figure 14).

A two-way RM ANOVA revealed a significant effect of time in f_B during exercise (p < 0.001). This effect was highlighted as a general increase from Ex-Pre to Ex-Post with across conditions (+4.3 breaths/min, p < 0.001)(Figure 14). Post hoc analysis for the significant effects of time in both $\dot{V}O_2$ (p = 0.023) and $\dot{V}CO_2$ (p = 0.004) revealed significant increases from Ex-Pre to Ex-Post across conditions ($\dot{V}O_2$: +0.04L/min, p = 0.023; $\dot{V}CO_2$: + 0.05L/min, p = 0.004).

The only respiratory variable to display a significant condition x time interaction effect during exercise was $P_{ET}O_2$ (p = 0.045). Post hoc analysis revealed significant increases from Ex-Pre to Ex-Post in both conditions, although this change was more than two-fold greater with IHc than time matched control (IHc: Δ3.16mmHg, p < 0.001; control: Δ1.45mmHg, p = 0.014). On the other hand, post hoc analysis for the main effect of time in $P_{ET}CO_2$ (p < 0.001) revealed significant decreases from Ex-Pre to Ex-Post across both conditions (-2.1mmHg, p<0.001).

Table 7. Average exercising ventilatory activity in room air across time and conditions.

	EXERCISE								
	Control			IHc			p-values		
	Ex-Pre	*Ex-Post*	*%Δ*	*Ex-Pre*	*Ex-Post*	*%Δ*	*Interaction*	*Condition*	*Time*
$\dot{V}_E$, L/min	*35.3 ± 6.5*	*39.3 ± 5.5*	*9%*	*33.9 ± 6.6*	*39.2 ± 4.1**	*15%*	***<0.001 (Friedman)***	*N/A*	*N/A*
f_B, breaths/min	*21 ± 4*	*25 ± 5**	*19%*	*21 ± 4*	*26 ± 5**	*23%*	*0.338*	*0.663*	***<0.001***
V_T, L	*1.7 ± 0.4*	*1.5 ± 0.4**	*-8%*	*1.7 ± 0.4*	*1.6 ± 0.3*	*-1%*	***<0.001 (Friedman)***	*N/A*	*N/A*
$\dot{V}O_2$, L/min	*1.1 ± 0.2*	*1.1 ± 0.2**	*2%*	*1.1 ± 0.2*	*1.1 ± 0.2**	*7%*	*0.107*	*0.666*	***0.022***
$\dot{V}CO_2$, L/min	*0.9 ± 0.2*	*1.0 ± 0.2**	*3%*	*0.9 ± 0.2*	*1.0 ± 0.2**	*10%*	*0.136*	*0.976*	***0.004***
$P_{ET}O_2$, mmHg	*103 ± 4*	*104 ± 4**	*1.5%*	*102 ± 5*	*105 ± 4**	*3.2%*	***0.045***	*0.536*	*<0.001*
$P_{ET}CO_2$, mmHg	*44 ± 5*	*42 ± 4**	*-5%*	*44 ± 4*	*42 ± 4**	*-4%*	*0.708*	*0.965*	***<0.001***
$\dot{V}_E$ / $\dot{V}_A$	*1.21± 0.05*	*1.23 ± 0.05*	*2%*	*1.22 ± 0.05*	*1.23 ± 0.07*	*1%*	*0.557*	*0.201*	*0.735*

*Values are mean ± SD. IHc, intermittent hypercapnia; $\dot{V}_E$, ventilation; f_B, frequency of breathing; V_T, tidal volume; $\dot{V}O_2$, volume of oxygen consumption; $\dot{V}CO_2$, volume of carbon dioxide consumption; $P_{ET}O_2$, partial pressure of end-tidal oxygen; $P_{ET}CO_2$, partial pressure of end-tidal carbon dioxide; $\dot{V}_A$, alveolar ventilation. * Significant effect of time ($p < 0.05$). † Significant effect of condition ($p < 0.05$).*

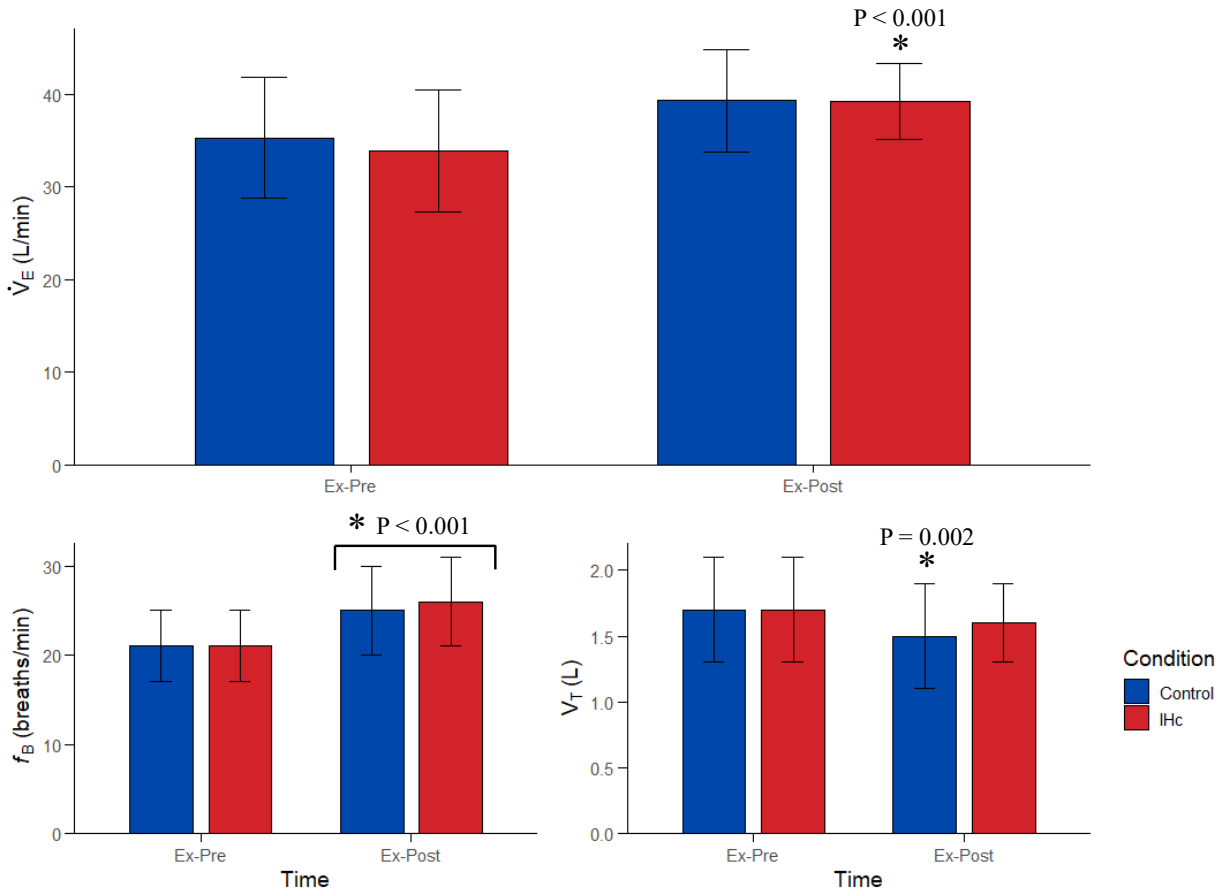


Figure 14. Average ± SD ventilation, breathing frequency, and tidal volume across time and conditions during exercise. $\dot{V}_E$ at Ex-Post appeared elevated from Ex-Pre with IHc (+4.9L/min, $p < 0.001$). An increase in f_B at Ex-Post from Ex-Pre was observed across conditions (+3.9 breaths/min) and IHc (+4.3 breaths/min, $p < 0.001$). V_T decreased significantly from Ex-Pre to Ex-Post with the control condition (-0.2L, $p = 0.002$) but not IHc. IHc, intermittent hypercapnia; $\dot{V}_E$, ventilation; f_B, frequency of breathing; V_T, tidal volume. * Significantly different from Pre ($p < 0.05$).

5.6 Changes in Resting PHC

Table 8 presents average baseline (pre-stimulus) respiratory values and responses to hypercapnic stimuli as the Δ between baseline and peak values. In alignment with findings reported in section 5.4 *The Control of Ventilation at Rest*, post hoc testing for main effects of time revealed increases from Pre to Post in baseline $P_{ET}O_2$ (+1.4mmHg, $p = 0.003$), baseline $\dot{V}_E$ (+1.7L/min, $p < 0.001$), and a coinciding decrease in baseline $P_{ET}CO_2$ (-2.1mmHg, $p < 0.001$).

Average ± SD PHC, with constituents $\Delta\dot{V}_E$ and $\Delta P_{ET}CO_2$ in response to hypercapnic stimuli are displayed in Figure 15. No significant effects were observed in resting PHC, $\Delta\dot{V}_E$, or $\Delta\dot{V}_I$ (%) in response to hypercapnic stimuli, although all three appeared to be approaching a significant condition x time interaction effect (PHC: $p = 0.077$; $\Delta\dot{V}_E$: $p = 0.081$; $\Delta\dot{V}_I$: $p = 0.069$). Meanwhile, a significant condition effect was observed for $\Delta P_{ET}CO_2$ ($p = 0.007$). Post hoc analysis showed $\Delta P_{ET}CO_2$ to be greater with control than IHc across both testing timepoints (control: + Δ1.2mmHg, $p = 0.007$).

Table 8. Average ventilatory output during 20s of baseline (pre-stimulus) and in response to PHC trials Pre and Post condition at rest.

	Rest Pre-Condition		***Rest Post-Condition***				
	CONTROL	*IHc*	*CONTROL*	*IHc*	*p-values*		
	Baseline (Pre- Stimulus)				*Interaction*	*Condition*	*Time*
$\dot{V}O_2$, L/min	*0.39 ± 0.48*	*0.29 ± 0.06*	*0.41 ± 0.46*	*0.29 ± 0.09*	*0.480*	*0.307*	*0.436*
$\dot{V}CO_2$, L/min	*0.23 ± 0.06*	*0.24 ± 0.06*	*0.26 ± 0.09*	*0.25 ± 0.07*	*0.575*	*0.844*	*0.180*
$P_{ET}O_2$, mmHg	*106.9 ± 5.1*	*107.1 ± 5.6**	*107.9 ± 4.6*	*108.9 ± 4.5 **	*0.452*	*0.537*	***0.003***
$P_{ET}CO_2$, mmHg	*40 .1 ± 3.7*	*39.7 ± 3.9**	*37.8 ± 3.9*	*37.8 ± 3.4 **	*0.433*	*0.739*	***<0.001***
$\dot{V}_E$, L/min	*14.9 ± 2.6*	*14.6 ± 2.6**	*16.6 ± 3.7*	*16.4 ± 1.9 **	*0.804*	*0.644*	***<0.001***
	Peripheral Hypercapnic Chemosensitivity Trials						
PHC, $L{\cdot}min^{-1}mmHg^{-1}$	*0.9 ± 0.4*	*0.8 ± 0.4*	*0.9 ± 0.4*	*1.0 ± 0.5*	*0.077*	*0.839*	*0.271*
Δ $\dot{V}_E$, L/min	*5.9 ± 3.5*	*4.1 ± 2.0*	*5.6 ± 3.7*	*5.2 ± 2.4*	*0.081*	*0.138*	*0.394*
Δ $P_{ET}CO_2$, mmHg	*6.9 ± 2.7 †*	*5.5 ± 1.9 †*	*6.7 ± 2.5*	*5.5 ± 2.3*	*0.683*	***0.007***	*0.628*
Δ $\dot{V}_I$, %	*31 ± 30*	*33 ± 33*	*23 ± 22*	*20 ± 11*	*0.069*	*0.719*	*0.182*
Δ f_B, %	*102 ± 100*	*86 ± 118*	*103 ± 122*	*106 ± 153*	*0.212 (Friedman)*	*N/A*	*N/A*
Δ $P_{ET}O_2$, %	*7 ± 5*	*7 ± 4*	*7 ± 3*	*6 ± 3*	*0.854 (Friedman)*	*N/A*	*N/A*
CV, %	*42 ± 23*	*36 ± 28*	*43 ± 23*	*42 ± 18*	*0.491*	*0.626*	*0.515*

*$\dot{V}O_2$, volume of oxygen consumption; $\dot{V}CO_2$, volume of carbon dioxide consumption; $P_{ET}O_2$, partial pressure of end-tidal oxygen; $P_{ET}CO_2$, partial pressure of end-tidal carbon dioxide; $\dot{V}_E$, ventilation; PHC, peripheral hypercapnic chemosensitivity; $\dot{V}_I$, volume of inspired air; f_B, frequency of breathing; CV, coefficient of variation; IHc, intermittent hypercapnia. * Significant effect of time ($p < 0.05$). † Significant effect of condition ($p < 0.05$).*

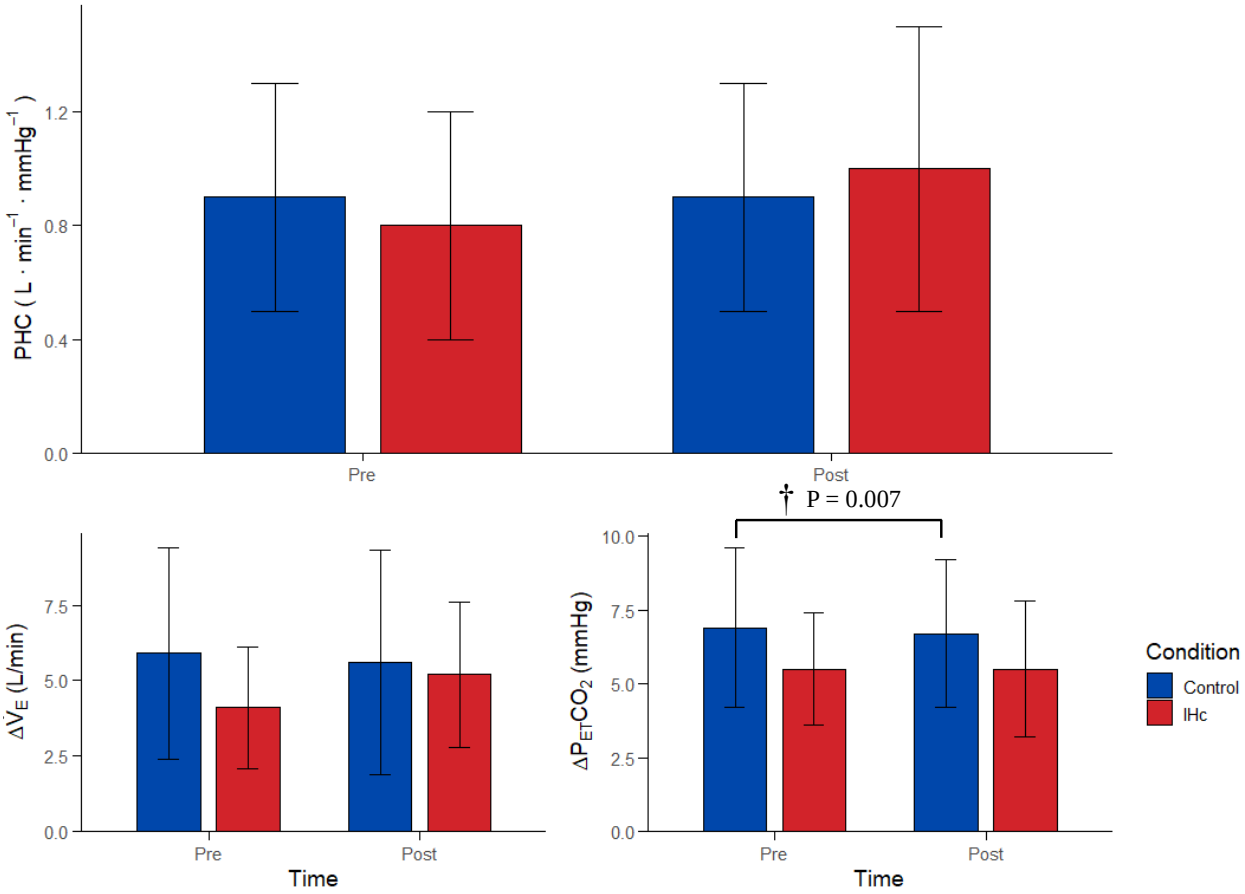


Figure 15. Average ± SD resting PHC, $\Delta P_{ET}CO_2$, and $\Delta \dot{V}_E$ across time and conditions. $\Delta P_{ET}CO_2$ was with control than IHc across testing timepoints (control: + Δ1.2mmHg, p = 0.007). IHc, intermittent hypercapnia; PHC, peripheral hypercapnic chemosensitivity; $\dot{V}_E$, ventilation; $P_{ET}CO_2$, partial pressure of end-tidal carbon dioxide. † Significant effect of condition ($p < 0.05$).

5.7 Changes in Exercising PHC

Table 9 presents the results from exercising PHC trials and corresponding pre-stimulus baselines in the exercising state. A significant condition x time interaction effect was observed in PHC responses during exercise (p = 0.011). Post hoc testing revealed a significant decline in PHC from Ex-Pre to Ex-Post with control (-0.19L·min^{-1}mmHg^{-1}, p = 0.017), contrary to the change in responses over time with IHc (+0.14L·min^{-1}mmHg^{-1}, p = 0.073). Despite the significant findings for PHC, constituents $\Delta \dot{V}_E$ and $\Delta P_{ET}CO_2$ showed no significant differences across times and conditions (Figure 16).

A significant condition x time interaction effect in pre-stimulus $\dot{V}_E$ ($p = 0.010$) aligns with findings reported *5.5 The Control of Ventilation during Exercise*, as post hoc testing highlighted significant increases from Ex-Pre to Ex-Post with IHc (Δ2.5L/min, $p < 0.001$) which were not observed with control (Δ0.87L/min, $p = 0.304$). A significant condition x time interaction effect was also observed in pre-stimulus $P_{ET}O_2$ ($p = 0.016$), although post hoc testing revealed no significant differences between the various time and condition groupings. Meanwhile, post hoc comparisons for the significant effect of time in pre-stimulus $P_{ET}CO_2$ ($p < 0.001$) showed consistent decreases from Ex-Pre to Ex-Post with across conditions (+2.4mmHg, $p < 0.001$).

Table 9. Average exercising ventilatory output during 20s of baseline (pre-stimulus) and in response to PHC testing across time and conditions.

	Exercise Pre-Condition		**Exercise Post-Condition**				
	CONTROL	*IHc*	*CONTROL*	*IHc*	*p-values*		
	Baseline (Pre- Stimulus)				*Interaction*	*Condition*	*Time*
$\dot{V}O_2$, L/min	*1.39 ± 1.29*	*1.08 ± 0.21*	*1.44 ± 1.50*	*1.08 ± 0.19*	*0.896 (Friedman)*	*N/A*	*N/A*
$\dot{V}CO_2$, L/min	*0.93 ± 0.19*	*0.96 ± 0.17*	*0.92 ± 0.22*	*0.94 ± 0.17*	*0.457 (Friedman)*	*N/A*	*N/A*
$P_{ET}O_2$, mmHg	*105.8 ± 4.3*	*105.4 ± 5.4*	*105.5 ± 4.1*	*106.4 ± 5.5*	***0.016***	*0.737*	*0.476*
$P_{ET}CO_2$, mmHg	*44.9 ± 4.5*	*44.5 ± 4.1**	*42.3 ± 3.9*	*42.2 ± 4.4**	*0.356*	*0.775*	***<0.001***
$\dot{V}_E$, L/min	*38.5 ± 5.4*	*37.6 ± 5.3*	*39.1 ± 5.4*	*40.2 ± 5.8 **	***0.010***	*0.936*	*0.007*
	Peripheral Hypercapnic Chemosensitivity Trials						
PHC, $L \cdot min^{-1} mmHg^{-1}$	*1.7 ± 0.8*	*1.4 ± 0.6**	*1.5 ± 0.7*	*1.6 ± 0.6*	***0.011***	*0.517*	*0.609*
$\Delta \dot{V}_E$, L/min	*15.1 ± 8.2*	*12.8 ± 6.2*	*13.6 ± 6.6*	*13.4 ± 8.3*	*0.213*	*0.448*	*0.458*
$\Delta P_{ET}CO_2$, mmHg	*10.5 ± 4.9*	*10.3 ± 5.3*	*10.3 ± 3.7*	*10.2 ± 5.5*	*0.884*	*0.900*	*0.687*
$\Delta \dot{V}_I$, %	*17 ± 10*	*16 ± 11*	*15 ± 9*	*14 ± 7*	*0.904*	*0.301*	*0.604*
Δf_B, %	*77 ± 107*	*72 ± 119*	*75 ± 121*	*71 ± 120*	*0.951*	*0.731*	*0.358*
$\Delta P_{ET}O_2$, %	*8 ± 4*	*8 ± 3*	*7 ± 4*	*6 ± 3*	*0.127 (Friedman)*	*N/A*	*N/A*
CV, %	*38 ± 20*	*35 ± 24*	*40 ± 28*	*42 ± 32*	*0.630*	*0.942*	*0.329*

*Values are mean ± SD. $\dot{V}O_2$, volume of oxygen consumption; $\dot{V}CO_2$, volume of carbon dioxide consumption; $P_{ET}O_2$, partial pressure of end-tidal oxygen; $P_{ET}CO_2$, partial pressure of end-tidal carbon dioxide; $\dot{V}_E$, ventilation; PHC, peripheral hypercapnic chemosensitivity; $\dot{V}_I$, volume of inspired air; f_B, frequency of breathing; CV, coefficient of variation. * Significant effect of time (p <0.05).* Significant effect of time (p < 0.05).† Significant effect of condition (p < 0.05).‡ Significant interaction effect of time and condition (p< 0.05).*

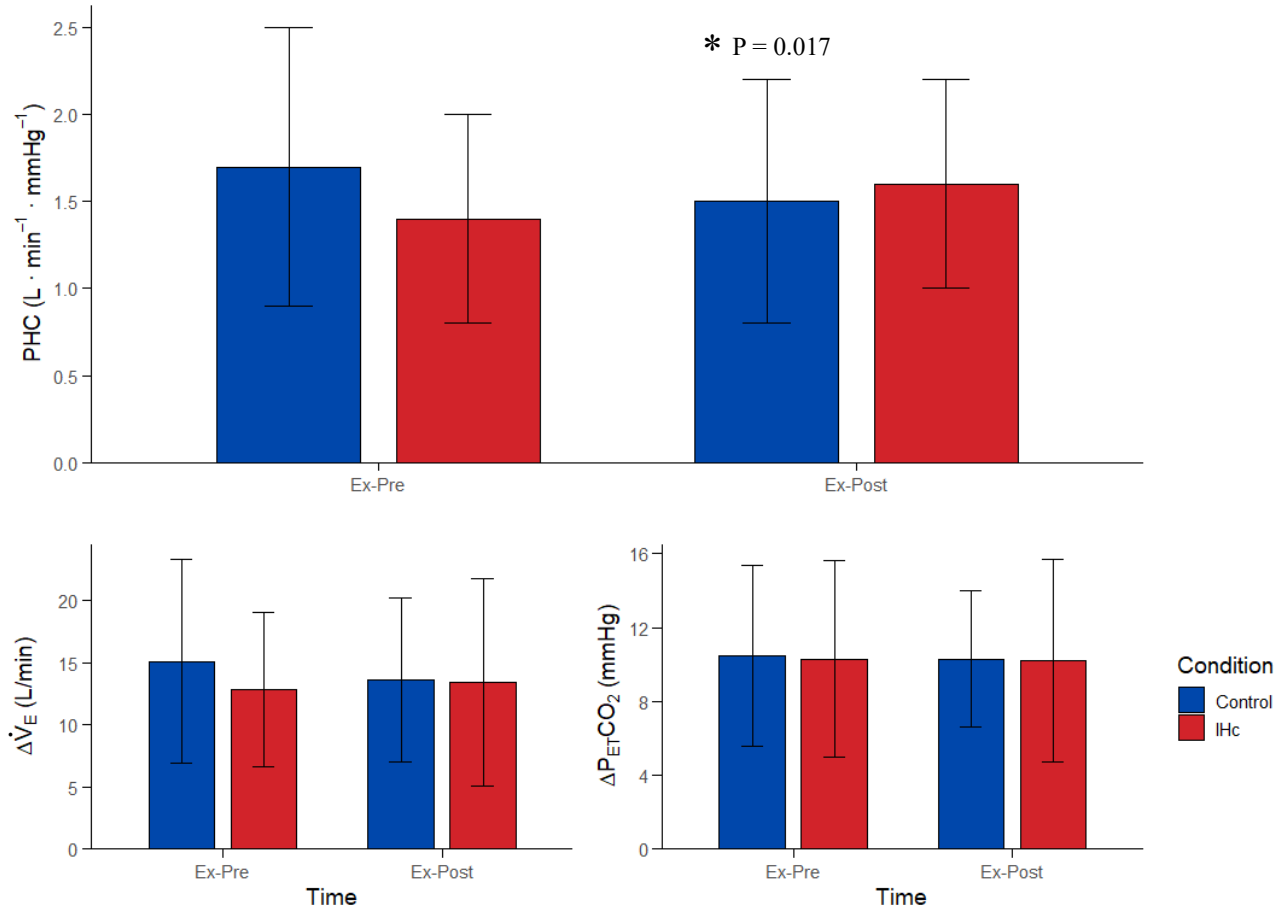


Figure 16. Average ± SD exercising PHC, $\Delta P_{ET}CO_2$, and $\Delta \dot{V}_E$ across time and conditions. PHC at Ex-Post was depressed relative Ex-Pre in the control condition (-0.19L·min^{-1}mmHg^{-1}, p = 0.017). IHc, intermittent hypercapnia; PHC, peripheral hypercapnic chemosensitivity; $P_{ET}CO_2$, partial pressure of end-tidal carbon dioxide; $\dot{V}_E$, ventilation. * Significantly different from Ex-Pre ($p < 0.05$).

5.8 Acute Responses to IHc

The following section reports findings from exploratory analysis into acute responses during the IHc protocol. Specifically, three different comparisons were made, as outlined in Figure 17: A) 20s vs 40s cycle averages between IHc vs. control (collapsed across the 30 minutes of condition), as reported in section *5.8.1*; B) Averages during the first vs. last 5 minutes of IHc vs. control (collapsed across 40s vs 20s cycles), as reported in section *5.8.2*; and C) Cycle-based changes (calculated as the

Δ between 40s hypercapnic cycles from preceding 20s normocapnic cycle) between the first and last 5 minutes of IHc, as reported in section *5.8.3*.

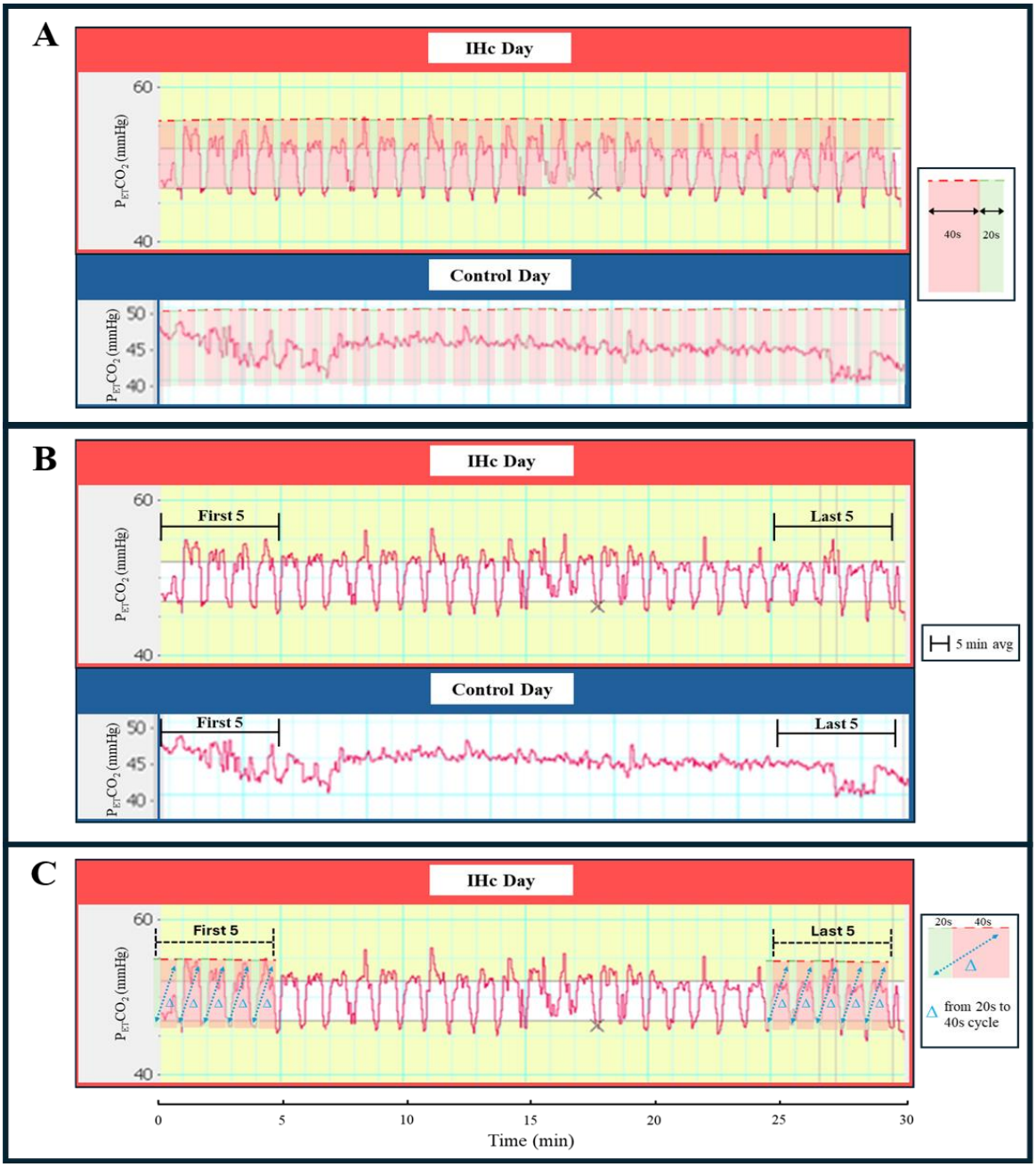


Figure 17. Overview of analytical comparisons made to evaluate acute responses to IHc. A) 20s vs 40s cycle averages between IHc vs. control; B) Averages during the first vs. last 5 minutes of IHc vs. control; and C) Δ between 40s hypercapnic cycles from preceding 20s normocapnic cycle between the first and last 5 minutes of IHc only.

5.8.1 Cha nges During 40s vs 20s Cycles Between Conditions

Average cardiorespiratory activity by cycle length and condition is presented in Table 10. Several significant interaction effects of condition x cycle length are reported. For $\dot{V}_E$, post hoc analysis for the significant interaction effect ($p < 0.001$) revealed elevations during the 40s cycles from the 20s cycles during IHc (Δ0.99L/min, $p < 0.001$) and no cycle-based changes during control (Δ0.15L/min, $p = 0.441$). With IHc, $\dot{V}_E$ appeared elevated from control during both the 40s and 20s cycles (40s: IHc + 7.75L/min, $p = 0.001$; 20s: IHc + 6.69L/min, $p = 0.004$). Interestingly, the only significant post hoc finding for the interaction effect in f_B ($p = 0.030$) revealed elevations during the 20s from the 40s cycles on the IHc day (Δ0.4 breaths/min, $p = 0.005$), with f_B appearing stable across cycles of control, and between conditions for each cycle. Similar findings appeared in post hoc testing for the interaction effect observed for $P_{ET}O_2$ ($p = 0.020$), whereby elevations occurred during the 20s from the 40s cycles during IHc (Δ0.826mmHg, $p < 0.001$) with no other significant differences found. Meanwhile, significant differences in $P_{ET}CO_2$ were observed across conditions and cycles, whereby 40s IHc cycles were elevated from 20s IHc cycles (Δ2.9mmHg, $p = 0.003$), 40s control cycles (Δ5.7mmHg, $p < 0.001$), and 20s control cycle (Δ5.54mmHg, $p < 0.001$) while remaining stable across cycles of control. Figure 18 summarizes cycle length driven changes as the %Δ in cardiorespiratory variables between 40s from 20s cycles by condition.

Further condition x cycle length interaction effects were found in SBP ($p = 0.032$) and MAP ($p = 0.013$), whereby elevations occurred during 40s from 20s cycles of IHc (SBP: Δ3.0mmHg; MAP: Δ1.9mmHg; both $p < 0.001$), and generally throughout IHc relative to control during both 40s cycles (SBP: Δ12.1mmHg, $p = 0.008$; MAP: Δ8.6mmHg, $p = 0.002$) and 20s cycles (SBP: Δ10.1mmHg, $p = 0.024$; MAP: Δ7.2mmHg, $p = 0.008$). Both SBP and MAP appeared stable across 40s and 20s cycles of control (SBP: Δ1.0mmHg, $p = 0.124$; MAP: Δ0.5mmHg, $p = 0.227$). No

interaction effect was observed for DBP, although there was a significant condition ($p = 0.022$) and cycle length ($p = 0.014$). Post hoc analysis revealed that DBP was generally greater with IHc than control across cycle lengths (IHc: + 5.7mmHg, $p = 0.022$), and during the 40s cycles relative to the 20s cycles across both conditions (40s: + 0.8mmHg, $p = 0.014$). Finally, HR showed only an effect of condition ($p = 0.028$), being generally elevated with IHc compared to control across 20s and 40s cycles (IHc: +10.3bpm, $p = 0.028$).

Table 10. Acute changes in cardiorespiratory activity between 40s and 20s cycles during IHc and control.

	Control			***IHc***			***p-values***		
	20s Cycle	*40s Cycle*	*%Δ*	*20s Cycle*	*40s Cycle*	*%Δ*	*Interaction*	*Condition*	*Cycle Length*
$\dot{V}_E$ (L/min)	39 ± 6	40 ± 6	-0.4	46 ± 10†	47 ± 10*†	2.2	**<0.001**	0.002	0.009
f_B (breaths/min)	24 ± 5	24 ± 5	-0.1	25 ± 5*	24 ± 5	-1.4	**0.030**	0.992	0.062
$P_{ET}O_2$ (mmHg)	106 ± 3	106 ± 3	-0.1	106 ± 5*	106 ± 6	-0.8	**0.020**	0.826	0.012
$P_{ET}CO_2$ (mmHg)	43 ± 4	43 ± 4	-0.3	46 ± 3†	49 ± 3 *†	6.5	**<0.001 (Friedman)**	N/A	N/A
HR (bpm)	108 ± 13	108 ± 13	0.2	117 ± 22†	117 ± 24†	0.2	0.350	**0.028**	0.082
SBP (mmHg)	147 ± 16	148 ± 17	0.7	157 ± 19†	160 ± 20 *†	1.9	**0.032**	0.014	<0.001
DBP (mmHg)	73 ± 10	73 ± 10	0.5	78 ± 12†	79 ± 12*†	1.6	0.100	**0.022**	**0.014**
MAP (mmHg)	95 ± 11	96 ± 11	0.5	102 ± 13†	104 ± 13*†	1.9	**0.013**	0.004	<0.001

Values are mean ± SD. IHc, intermittent hypercapnia; $\dot{V}_E$, ventilation; f_B, frequency of breathing; $P_{ET}O_2$, partial pressure of end-tidal oxygen; $P_{ET}CO_2$, partial pressure of end-tidal carbon dioxide; HR, heart rate; SBP, systolic blood pressure; DBP, diastolic blood pressure, MAP, mean arterial pressure.). Significant effect of cycle length ($p < 0.05$).† Significant effect of condition ($p < 0.05$).*

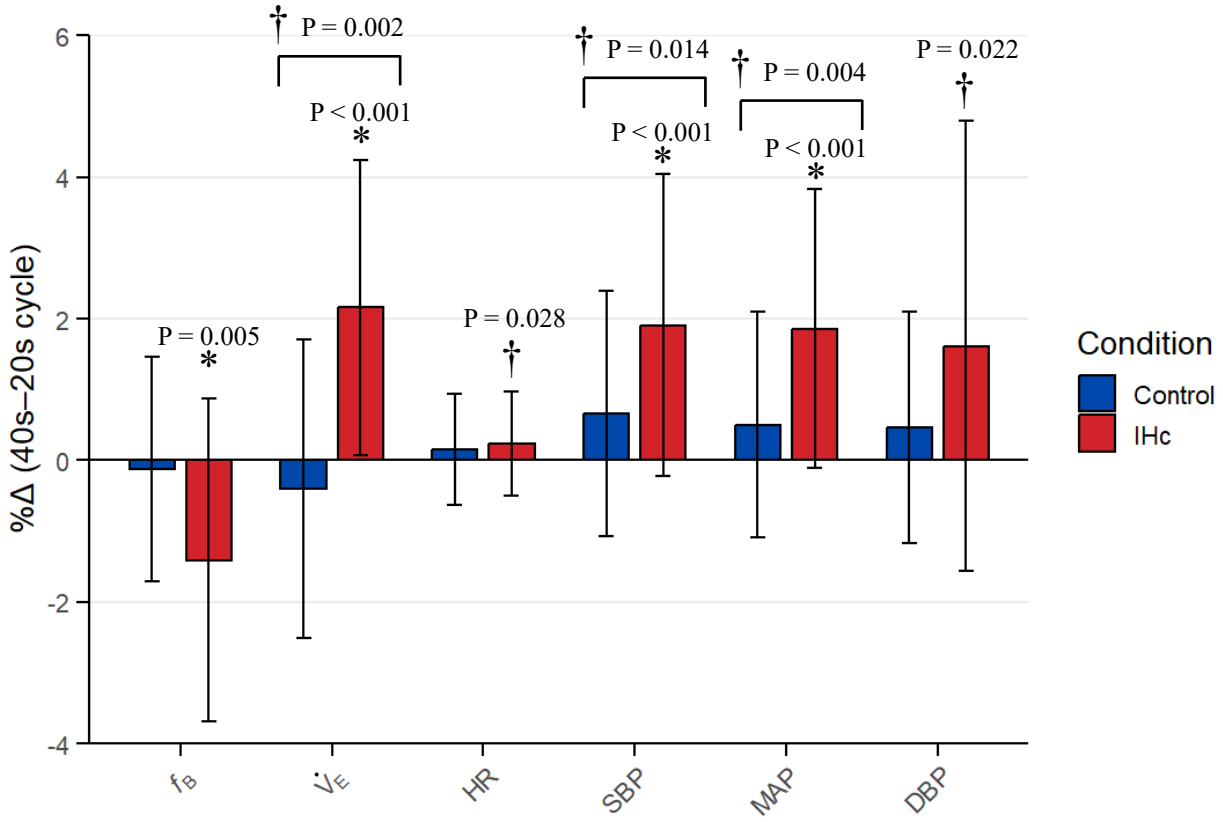


Figure 18. Mean ± SD percent change from 20s to 40s cycles by condition. f_B was elevated during 20s cycles from 40s cycles with IHc (20s: +0.4 breaths/min, p = 0.005). $\dot{V}_E$ was elevated with IHc relative to control across both cycle lengths (p = 0.002), as well as during 40s cycles of IHc relative to 20s cycles (40s: +1L/min, p < 0.001). HR and DBP were elevated with IHc relative to control across both cycle lengths (HR: 10.3bpm, p = 0.028; DBP: + 5.7mmHg, p = 0.022). SBP and MAP were elevated during 40s cycles of IHc relative to 20s cycles of IHc (SBP: +3mmHg, p < 0.001; MAP: +2mmHg, p < 0.001), as well as generally with IHc compared to control across both cycle lengths (SBP: p = 0.014; MAP: p = 0.004). IHc, intermittent hypercapnia; $\dot{V}_E$, ventilation; f_B, frequency of breathing; HR, heart rate; SBP, systolic blood pressure; DBP, diastolic blood pressure, MAP, mean arterial pressure.* Significant effect of cycle length (p < 0.05). † Significant effect of condition (p < 0.05).

5.8.2 Changes from the First to Last 5- Minutes during IHc and Control

Table 11 reports average cardiorespiratory activity over the course of the first and last 5 minutes of IHc and control. Figure 19 summarizes time-based changes, calculated as the %Δ from the first to the last 5 minutes by condition. Post hoc analysis for the significant condition x time interaction in $\dot{V}_E$ (p = 0.001) revealed IHc deviated from time-matched control in the last 5 minutes

(IHc: + 9.4L/min, $p < 0.001$) despite not being significantly different in the first 5 minutes (IHc: +3.4L/min, $p = 0.108$). In alignment, $\dot{V}_E$ increased by 6.8L/min over time with IHc ($p < 0.001$) while remaining stable with control (Last 5: +0.8L/min, $p = 0.476$). On the other hand, post hoc analysis for the significant interaction effect in f_B ($p = 0.048$) showed similar increases from the first to last 5 minutes across both conditions (IHc: +3.2 breaths/min; control: + 2.1 breaths/min; both $p < 0.001$) with no significant differences between conditions at either time point. As expected, a significant condition x time interaction effect was observed for $P_{ET}CO_2$, with post hoc analysis highlighting measurements during IHc as +4.0mmHg and +5.2mmHg higher than time matched control during the first and last 5 minutes, respectively (both $p < 0.001$). Additionally, a time effect was observed for $P_{ET}CO_2$ within control (Last 5: -1.7mmHg, $p < 0.001$) but not IHc (Last 5: -0.5mmHg, $p = 0.119$). $P_{ET}O_2$ appeared stable across conditions and over time.

Post hoc analysis for the significant condition x time interaction effect in HR ($p = 0.008$) revealed elevations with IHc vs control in the last 5 minutes of condition (IHc: + 7.4bpm, $p = 0.031$) despite there being no significant differences in the first 5 minutes (IHc: + 2.9bpm, $p = 0.361$). This was also captured as a significant effect of time in IHc (Last 5: + 6.4bpm, $p < 0.001$) while appearing stable with control (Last 5: + 1.9bpm, $p = 0.144$). Similarly, an interaction effect in SBP ($p = 0.026$) showed significant deviations between conditions in the last 5 minutes (IHc: +18mmHg, $p = 0.01$) despite no differences in the first 5 minutes (IHc: +8mmHg, $p = 0.090$), as found by post hoc testing. This is partially accounted for by a significant decrease in SBP from the first to last 5 minutes of control (Last 5: -7mmHg, $p = 0.009$), which was unmatched with IHc (Last 5: +3mmHg, $p = 0.308$). Meanwhile, post hoc analysis for the condition-effect observed in MAP ($p < 0.001$) revealed a 10mmHg elevation with IHc relative to control across both time points ($p < 0.001$). Likewise, a

significant condition-effect in DBP (p = 0.002) showed an 8mmHg elevation with IHc relative to control across both time points, with no effect of time.

Table 11. Average ± SD cardiorespiratory activity over the course of the first and last 5 minutes by condition

	Control			***IHc***			***p-values***		
	First 5	*Last 5*	*%Δ*	*First 5*	*Last 5*	*%Δ*	*Interaction*	*Condition*	*Time*
$\dot{V}_E$ (L/min)	39 ± 5	39 ± 6	2%	42 ± 10	49 ± 10*†	18%	**0.001**	0.003	<0.001
f_B (breaths/min)	23 ± 4	25 ± 5*	9%	23 ± 5	25 ± 6*	14%	**0.048**	0.443	<0.001
$P_{ET}O_2$ (mmHg)	107 ± 4	106 ± 4	-1%	107 ± 6	107 ± 14	1%	0.426	0.992	0.568
$P_{ET}CO_2$ (mmHg)	44 ± 4	42 ± 4*	-4%	48 ± 3†	48 ± 4†	-1%	**0.018**	<0.001	<0.001
HR (bpm)	107 ± 12	109 ± 14	2%	112 ± 19	119 ± 26*†	16%	**0.008**	0.112	0.001
SBP (mmHg)	152 ± 17	145 ± 19*	-5%	160 ± 20	162 ± 23†	2%	**0.026**	0.004	0.178
DBP (mmHg)	73 ± 10	70 ± 11	-4%	79 ± 13†	80 ± 15†	2%	0.085	**0.002**	0.434
MAP (mmHg)	97 ± 12	93 ± 13	-4%	104 ± 14†	105 ± 16†	1%	0.094	**<0.001**	0.193

Values are mean ± SD. IHc, intermittent hypercapnia; $\dot{V}_E$, ventilation; f_B, frequency of breathing; $P_{ET}O_2$, partial pressure of end-tidal oxygen; $P_{ET}CO_2$, partial pressure of end-tidal carbon dioxide; HR, heart rate; SBP, systolic blood pressure; DBP, diastolic blood pressure, MAP, mean arterial pressure.). Significant effect of cycle length ($p < 0.05$).† Significant effect of condition ($p < 0.05$).*

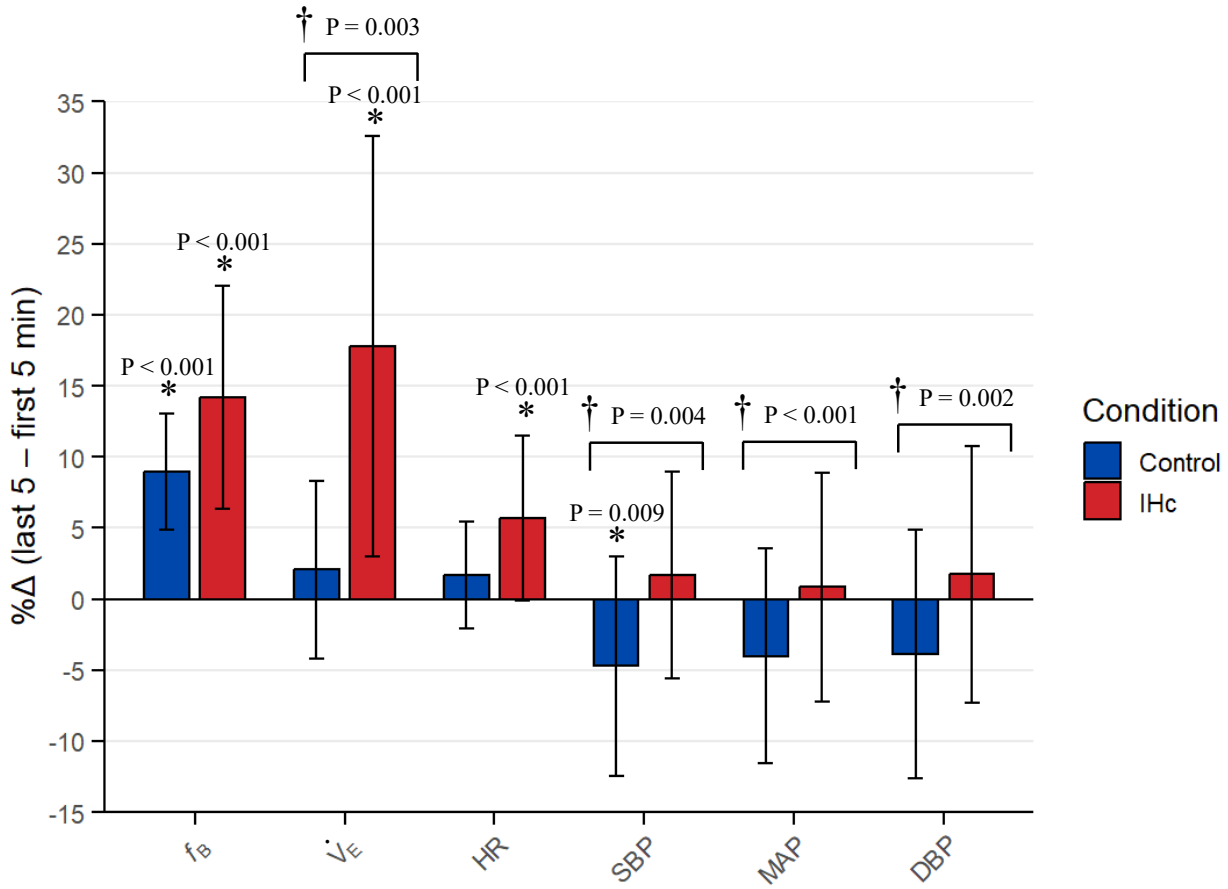


Figure 19. Mean ± SD percent change from the first to last 5 minutes of condition. f_B increased from the first to last 5 minutes within control and IHc (both $p < 0.001$). With IHc, $\dot{V}_E$ increased significantly from the first to last 5 minutes ($p < 0.001$) and was generally elevated from time-matched control ($p = 0.003$). HR increased from the first to last 5 minutes of IHc ($p < 0.001$). SBP significantly decreased from the first to last 5 minutes of control ($p = 0.009$). SBP, DBP, and MAP all appeared generally elevated with IHc relative to time matched control (SBP: $p = 0.004$; MAP: $p < 0.001$; DBP: $p = 0.002$). IHc, intermittent hypercapnia; f_B, breathing frequency; $\dot{V}_E$, ventilation; HR, heart rate; SBP, systolic blood pressure; MAP, mean arterial pressure; DBP, diastolic blood pressure.* Significant effect of time ($p < 0.05$). † Significant effect of condition ($p < 0.05$).

5.8.3 Differences in the Magnitude of Response to Hypercapnia (Δ40s-20s) over the course of IHc

Final analysis evaluated differences in the response to 40s hypercapnic cycles (Δ from preceding 20s normocapnic cycle) between the first and last 5 minutes within the IHc condition. In response to 40s hypercapnic cycles, $\Delta\dot{V}_E$ from increased from the first to last 5 minutes of IHc (Last 5: +1L/min, $p = 0.007$). Similarly, $\Delta P_{ET}CO_2$ increased by 0.8mmHg over the course of IHc ($p =$

0.041). To evaluate varying responsiveness between variables across time, %Δ from the first to last 5 minutes was calculated for $\Delta\dot{V}_E$ and $\Delta P_{ET}CO_2$ and is displayed in Figure 20. A Pearson correlation test revealed no correlation between the Δ% in $\Delta\dot{V}_E$ and $\Delta P_{ET}CO_2$ over time (r = 0.002).

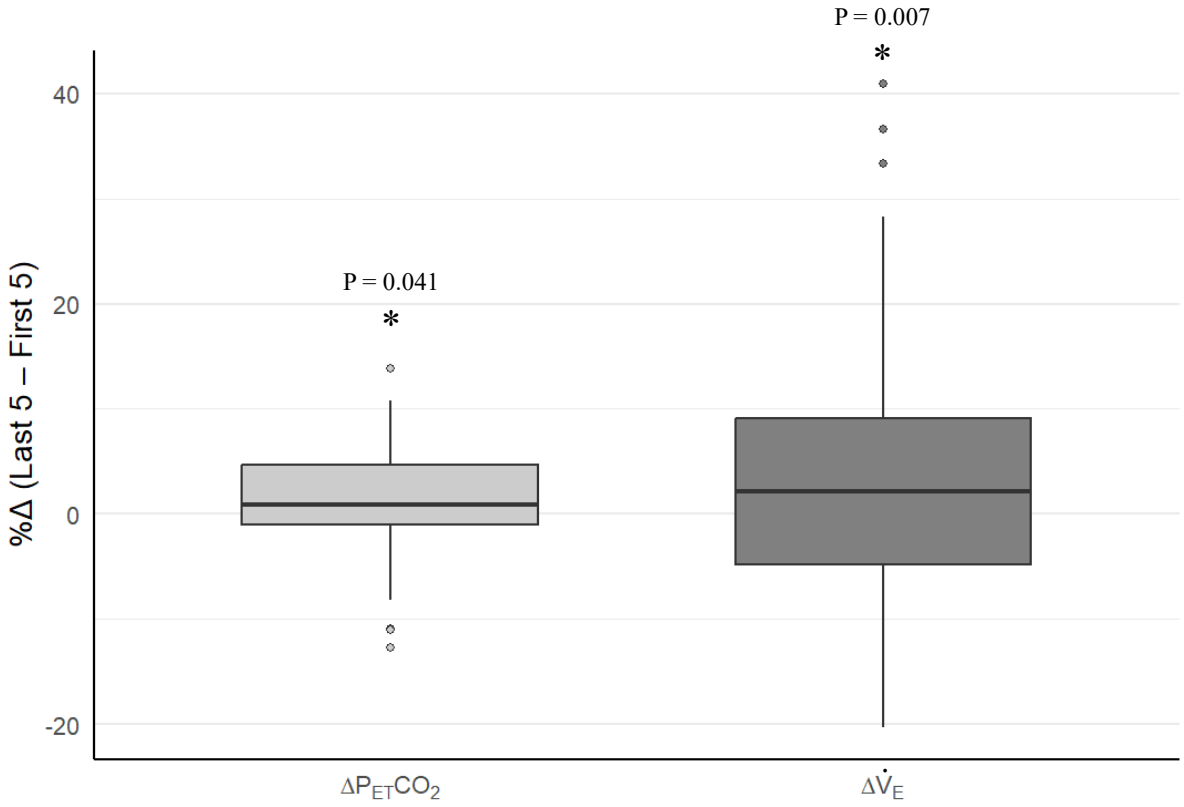


Figure 20. Changes in $\Delta\dot{V}_E$ and $\Delta P_{ET}CO_2$ in response to hypercapnic cycles over the course of IHc, calculated as the %Δ from the first to the last 5 minutes. Both $\Delta\dot{V}_E$ and $\Delta P_{ET}CO_2$ increased from the first to last 5 minutes of IHc ($\Delta\dot{V}_E$: p = 0.007; $\Delta P_{ET}CO_2$: p = 0.041). IHc, intermittent hypercapnia; $\dot{V}_E$, ventilation; $P_{ET}CO_2$, partial pressure of end-tidal carbon dioxide. * Significant effect of time (p < 0.05).

Chapter 6
Discussion

6.1 Main Findings

The present study evaluated the physiological effects of IHc in combination with moderate-intensity exercise on cardiovascular function and the control of $\dot{V}_E$ in the exercising and resting state. Specifically, I addressed two primary research questions: 1) Will resting MAP at Post, Post-25, and Post-35 be elevated from Pre following IHc in comparison to time-matched control?, and 2) Will resting $\dot{V}_E$ be depressed Post relative to Pre following IHc in comparison to time-matched control? To evaluate the involvement of peripheral chemoreceptors in the anticipated modulation of cardiorespiratory activity following IHc, we also sought to determine if the PHC at Post was elevated from Pre 3) during exercise, and 4) at rest following exposure to IHc relative to time-matched control.

The main findings of this study are threefold. First, although MAP was not significantly elevated across the 35-minute resting period, exercising MAP increased significantly from Ex-Pre to Ex-Post while showing no differences across time with control (Figure 12). Significant increases in HR with IHc which were not reflected in the time-matched control were also observed during exercise (Figure 12) and at rest (Figure 11). These findings suggest that exercise may modulate plastic facilitation of cardiovascular activity following IHc.

Second, IHc led to an increase in $\dot{V}_E$ in comparison to control, both at rest (Figure 13) and during exercise (Figure 14), although only disproportionately to metabolic demand at rest. Additionally, exercising PHC following IHc deviated from the time-matched control (Figure 16). These changes suggest the presence of vLTF following IHc during exercise, potentially via sensory LTF, and that the expression of functional plasticity may be modulated by exercise.

Finally, $\Delta\dot{V}_E$ in response to the 40s hypercapnic cycles (% change from preceding normoxic cycle) increased from the first to last 5-minutes of IHc and was disproportionate to $\Delta P_{ET}CO_2$ (Figure 20). This dissociation between stimulus and response may demonstrate a progressive sensitization that precedes the emergence of sensory LTF.

To our knowledge, this is the first study to demonstrate vLTF following IHc without concurrent hypoxia. Overall, the observed effects appear to be predominantly driven by increases in peripheral chemoreceptor and sympathetic activity. The timing and expression of vLTF appeared modulated by physiological state (resting vs exercising), possibly due to an initial masking by Ex-Post exercise homeostatic suppressive mechanisms until excitatory drive surpassed inhibitory factors.

6.2 Implications for Cardiovascular Regulation

6.2.1 Blood Pressure and Autonomic Modulation

We hypothesized that resting MAP would be significantly elevated from pre throughout the 35-minute seated period in room air following IHc compared to time matched control. Contrarily, no effects of condition or time were observed for MAP, nor SBP (Figure 11). The only significant effect found in resting BP was a general effect of time in DBP, which was elevated at Post-25 from Pre across both conditions (Post-25: + 4.4mmHg, $p = 0.050$) (Figure 11). Therefore, IHc was not found to influence BP at rest, which contradicts findings in the literature. Using 40-minutes of the same IHc protocol employed in the current study, although in the absence of exercise, Shing et al., (2025) reported a 6.1mmHg increase in MAP from pre to post-IHc whereas the current study observed a 1.4mmHg increase (7). This discrepancy suggests that the added physiological stimuli of exercise may modulate plastic changes following IHc. During exercise, MAP decreased significantly from pre to post IHc, contrary to responses during time-matched control which showed no significant changes over time (IHc: -7 ± 12%; control: -5 ± 11%)(Figure 12). This was not reflected in exercising SBP or

DBP, which responded similarly in magnitude between conditions despite DBP appearing 4.7mmHg higher than control across both IHc time points ($p = 0.043$).

The lack of significant BP findings at rest following IHc, in combination with the significant effect observed in exercising MAP, is suggestive of exercise modulating the formation or expression of plasticity facilitating vascular function. A possible mechanism to which exercise could modulate the BP response to IHc is the interplay between the effects of exercise and hypercapnia on baroreceptors. Willie et al., (2011) found reduced baroreflex sensitivity following exercise to be attributable to changes in both autonomic and vascular modulation and resulting in hysteresis to rising or falling BP (59). On the other hand, hypercapnia (5% CO_2) has been observed to increase resting BP and the baroreflex 'set-point' up to 60 minutes Ex-Postposure (60). Lastly, Yamashiro et al., (2024) recently reported that the expression of LTF induced by a combination of CO_2 and exercise is based on a balance between self-excitatory and self-inhibitory neuronal pools, where LTF is expressed once excitatory chemoreceptor drive exceeds homeostatic suppressive forces (61).

To conclude, the expected resting BP response to IHc, specifically in MAP, was absent throughout 35-minutes of rest when the IHc protocol was administered during exercise. The exaggerated drop in exercising MAP with IHc relative to control suggests that exercise may modulate the formation of plastic changes, but that they might not be fully abolished. Findings in the literature support exercise as a homeostatic suppressive force which could mask functional expression of LTF, although it is unascertainable whether the expected rise in resting MAP following IHc was abolished, delayed, or attenuated in the current study.

6.2.2 Evidence for Sympathetic LTF

In both the resting and exercising state, significant increases in HR were observed from pre to post IHc, which were more than double the responses observed with control (Figure 11 & 12). This response likely reflects enhanced sympathetic activation, diminished parasympathetic (vagal) modulation, or a combination of both. While direct measurements of SNA were not conducted, the persistent HR elevation suggests the occurrence of sympathetic LTF.

The increased HR is consistent with previous demonstrations of sustained elevations in sympathetic outflow following IH in the presence of CO_2 (1, 48, 49). In some cases, sympathetic LTF has been found to manifest without significant changes in arterial pressure, although usually accompanied by phrenic LTF (48, 50, 51, 52). Also, denervation of the CB has been found to attenuate both phrenic and sympathetic LTF following IH with CO_2, although not fully abolished (30, 53). Although the exact mechanisms and interplay underlying sensory and sympatho-adrenal excitatory plastic enhancements are not fully understood, afferent input and central processing are thought to play a large role (50, 51).

In the context of our study, the additional stimuli of exercise during IHc may have influenced the manifestation of sympathetic LTF. Brain-derived neurotropic factor (BNDF) is known to play a role in plastic changes initiated by central chemoreceptors (54). Although CSF was unlikely to have been impacted by the duration of CO_2 exposure in the current study, exercise is also known to upregulate BNDF and promote plastic changes and may have enhanced sympathetic facilitation (55). Collectively, these findings extend existing evidence highlighting CO_2 as a potent modulator of autonomic function, potentially driving adaptive (or maladaptive) cardiovascular responses during recovery from exercise (7, 56).

6.3 The Impact of IHc and Exercise on Ventilatory Control and Plasticity

6.3.1 Primary Indicators of Sensory LTF

Significant increases in exercising PHC were observed following IHc in comparison to time matched control. From pre to post condition, exercising PHC increased by 14% (± 25) with IHc, while decreasing by -8% (± 20) with control (Figure 16). The increase in PHC following IHc is a hallmark feature sensory LTF, reflecting enhanced afferent signaling from the CB to central respiratory centers. Enhancements may also occur centrally within the NTS, facilitating afferent integration and respective efferent outputs (72). While PHC can exhibit short-term variability, the magnitude and direction of change observed with IHC in comparison to time matched control are consistent with true physiological adaptations rather than noise.

This enhanced chemosensitivity is consistent with previously demonstrated models of sensory LTF (62, 63). While the mechanisms and interplay involved CB afferent facilitation are yet to be fully understood, previous studies have implicated enhanced presynaptic neurotransmitter release (e.g., ATP, dopamine) from type I glomus cells (64, 65), upregulation of ROS (62, 63), and serotonin-mediated signaling involving 5-HT_2 receptor activation (66, 67). Together, these findings point towards a functional upregulation of peripheral chemoreceptor output following IHc. The consistent directionality across both rest and exercise suggests that sensory plasticity was expressed across physiological states, potentially facilitating downstream ventilatory adjustments.

6.3.2 Secondary Evidence for Sensory LTF

Although the observed enhancement in PHC appeared to translate into a functional increase in $\dot{V}_E$, which increased significantly from Ex-Pre to Ex-Post with IHc (+15% ± 11, $p < 0.001$) but not with control (Figure 16), $\dot{V}_E/\dot{V}CO_2$ and $\%\Delta\dot{V}_E/\%\Delta\dot{V}CO_2$ did not differ between conditions which

suggests that the increased $\dot{V}_E$ during exercise was proportionate to metabolic demand. However, condition-driven differences in $\dot{V}_E$ responses over time persisted into resting observation (IHc: +17% ± 21, $p < 0.001$ vs control: +13% ± 23, $p > 0.05$) (Figure 13), with significant differences in $\%\Delta\dot{V}_E/\%\Delta\dot{V}CO_2$ between conditions becoming apparent (IHc: 0.4 ± 2.6; control: 1.0 ± 1.2; $p= 0.03$). This divergence suggests that $\dot{V}_E$ became uncoupled from metabolic drive at rest, potentially reflecting a short-term suppression of respiratory drive following IHc upon returning to the resting state.

The apparent varying degrees of vLTF expression during exercise and rest may reflect a state-dependent manifestation of respiratory plasticity. Yamashiro *et al*., (2024) proposed that excitatory chemoreceptor input following intermittent CO_2 exposure may be integrated over time, with LTF becoming functionally expressed only after a threshold of excitatory drive surpasses homeostatic suppression (61). It is possible that exercise-induced activation of central command or mechanoreflex pathways heightened the excitability of respiratory circuits and allowed the functional expression of chemosensory plasticity (61). Thus, exercise may act as a permissive state for the expression of vLTF by shifting the balance toward excitatory dominance, overcoming suppressive influences that may otherwise mask facilitation during rest.

Although vLTF is often characterized by a delayed and gradual emergence, the resting measurement in the present study (~12–15 minutes post-IHc) may have occurred too early to capture the full expression of facilitation. Additionally, the transition from exercise to rest is accompanied by transient autonomic adjustments that may relatively suppress ventilatory drive. While overt hypotension was not observed in the current study, previous research has shown that Ex-Post exercise hypotension — typically characterized by reductions in sympathetic vasomotor tone and baroreflex resetting — can blunt chemoreflex sensitivity and respiratory motor output (59, 68). Although all

measurements in the present study were conducted in the seated position, where such effects may be attenuated, similar mechanisms could have transiently influenced ventilatory drive during early recovery. These effects may temporarily oppose the excitatory influence of increased chemosensitivity, effectively masking the early expression of vLTF. Furthermore, inhibitory afferent input via baroreceptor activation has been shown to suppress phrenic nerve output (69), offering a potential mechanism by which IHc-induced plasticity could be functionally constrained during early recovery. Taken together, these findings suggest that the differing expression of vLTF across states may reflect a dynamic interplay between the timing of plasticity onset and the prevailing balance of excitatory and inhibitory inputs to the respiratory network.

The lack of change in exercising V_T following IHc, which contradicted the significant decline following time-matched control (-0.2L, $p = 0.002$) (Figure 14), may offer further insight into the expression of vLTF. A shift in breathing patterns towards deeper, more efficient breaths is a hallmark feature of respiratory motor plasticity in both human and animal models (70,71). The lack of significant change in exercising V_T, contrary to the time-matched control, may represent preservation. Furthermore, the lack of significant difference in resting V_T between IHc and control supports the idea of state-dependent expression of plasticity.

It is also possible that plasticity occurred not only at the level of the CB, but also within the central integrative circuits of the brainstem. Prior research has demonstrated that intermittent hypercapnia or hypoxia can induce synaptic plasticity within the NTS, enhancing the integration of CB input and facilitating downstream ventilatory output (72). While the present study does not directly measure synaptic changes within the brainstem, the preserved V_T and elevated PHC suggest a coordinated sensory-to-motor facilitation that may be mediated in part by such integrative mechanisms. This highlights the possibility of a third domain of vLTF expression — distinct from

purely afferent or efferent adaptations — in which plasticity within central relay nuclei contributes to respiratory motor facilitation.

Altogether, these findings highlight the complexity of vLTF as a distributed, state-dependent phenomenon shaped by the interplay of multiple physiological systems. The expression of vLTF is not determined solely by the presence of plasticity at a single site, but rather by how peripheral chemoreceptor sensitization, central integrative processing, and respiratory motor output interact with dynamic modulatory influences — including baroreflex inhibition, central command activation, and metabolic feedback (61, 66, 69, 72, 73). The fact that distinct patterns emerged during exercise and rest underscores the importance of evaluating vLTF within the context of physiological state, temporal dynamics, and systemic crosstalk. While sensory plasticity appeared to be the primary driver in the present study, its expression was likely modulated by transient autonomic adjustments, integrative gain in brainstem circuits, and breathing pattern compensation. Together, these findings reinforce the view that vLTF represents an emergent property of the integrated respiratory control system, with its manifestation dependent not only on the nature of the stimulus, but also on the broader regulatory environment in which it is expressed.

6.4 Differences in Cycle-Driven Effects between Conditions

While prior sections examined Pre- and Post-condition averages under room air breathing, these comparisons do not capture the evolving physiological responses that occur during IHc exposure itself. The following section explores acute cycle-based effects across time, focusing on how the cardiorespiratory system responded to hypercapnic stimuli both within and across the 30-minute IHc protocol. This analysis provides insight into the immediate physiological consequences of repeated hypercapnic stimulation and highlights time-dependent patterns that may reflect early plasticity. Specifically, we examine: (1) acute physiological responses during IHc versus control

(*Section 6.4.1*); (2) time-dependent changes between 5-minute averages at the beginning and end of conditions (*Section 6.4.2*); and (3) progressive amplification over the course of IHc of ventilatory responsiveness to 40s hypercapnic cycles from normoxia, suggesting early-stage chemosensory gain (*Section 6.4.3*).

6.4.1 Acute Effects During 40s vs 20s Cycles Between Conditions

Significant cycle × condition interactions revealed that IHc—but not control—elicited robust increases in $\dot{V}_E$, f_B, SBP, and MAP during 40-second hypercapnic cycles compared to interspersed normocapnic periods (Figure 18). These findings confirm that IHc exposure produced effective fluctuations in blood gas levels to trigger adjustments in cardiorespiratory output. The modest elevations in $P_{ET}O_2$, although unexpected due to ETF clamping, likely reflect carryover effects from preceding hypercapnic cycles rather than true oxygen perturbation, and fall within the physiological range of arterial saturation (74). Notably, the absence of such ventilatory modulation in the control condition reinforces the specificity of the hypercapnic stimulus. This pattern suggests that even within early cycles, chemoreceptor activation and reflexive ventilatory adjustments were engaged — setting the stage for progressive adaptations with repeated stimulation (61,75,76).

The concurrent elevations in SBP, MAP, and to a lesser extent DBP during IHc cycles support the idea that acute hypercapnia activated sympathetic vasoconstrictor pathways via peripheral chemoreflex activation (66,76)(Figure 18). HR remained relatively unchanged, consistent with baroreflex buffering of cardiac responses to elevated BP (69). These effects highlight the interplay between chemoreceptor input and baroreflex modulation, particularly under conditions where CO_2 acts as a potent excitatory stimulus for sympathetic outflow (77). While contributions from muscle metaboreflex pathways are typically observed during prolonged exertion or sustained metabolite accumulation (78,79), their role here was likely minimal due to rapid CO_2 clearance and interspersed

normocapnic recovery. The acute cardiovascular profile observed during IHc cycles thus likely reflects the combined effects of chemoreflex activation and reflex inhibition, modulated by autonomic integration.

6.4.2 Time -Dependent Changes Across the First and Last 5-Minutes (Between Conditions)

When averaged across the first and final 5-minutes of IHc exposure, both HR and $\dot{V}_E$ exhibited significant increases, while no change was observed under control conditions (Figure 19). This cumulative shift is suggestive of gradually accumulating autonomic and ventilatory engagement, consistent with progressive changes in respiratory and sympathetic output observed across the IHc exposure period. The progressive increase in HR may reflect sustained sympathetic excitation, while the concurrent rise in $\dot{V}_E$ suggests an enhancement in ventilatory drive, possibly mediated by sensory LTF or by plasticity within integrative circuits of the brainstem responsible for processing chemosensory input (72,80). In contrast, the control condition exhibited reductions in SBP and MAP over time, indicative of typical cardiovascular drift during prolonged low-intensity activity (73). These contrasting patterns point toward a cumulative physiological shift unique to repeated IHc exposure, distinct from passive recovery or metabolic drift. Although typical indices such as $\dot{V}_E/\dot{V}CO_2$ or $\%\Delta\dot{V}_E/\%\Delta\dot{V}CO_2$ are useful in distinguishing metabolic versus plastic ventilatory effects, such comparisons are inappropriate in the present context due to the deliberate manipulation of end-tidal CO_2 during the IHc condition. As $\dot{V}CO_2$ could not be accurately measured during ETF, and $P_{ET}CO_2$ was artificially elevated by design, $\dot{V}_E$ cannot be directly normalized to a metabolic signal. As such, the observed increase in $\dot{V}_E$ over time is interpreted not as a response to rising metabolic demand, but rather as an emergent property of progressive chemoreceptor engagement and possible plastic gain within ventilatory control circuits (72,80).

6.4.3 Phasic Amplification of the Acute Hypercapnic Response Over Time (Within IHc only)

To explore whether responsiveness to hypercapnic stimuli changed over the course of IHc, ventilatory responses to the 40-second hypercapnic phases were compared between the first and final five minutes of exposure. A progressive increase in $\Delta\dot{V}_E$ was observed over time, despite only modest and controlled elevations in $P_{ET}CO_2$, suggesting that a relatively stable chemical stimulus elicited an increasingly robust ventilatory response (Figure 20).

To determine whether this pattern reflected changes in metabolic drive or altered chemosensory responsiveness, additional analyses were conducted. The relative changes in $\dot{V}_E$ and $P_{ET}CO_2$ (%Δ from preceding normocapnic phases) were compared across participants, and the slope of %Δ $\dot{V}_E$ /%Δ $P_{ET}CO_2$ was calculated for each time point. No significant correlation was observed between the magnitude of the CO_2 stimulus and the ventilatory response ($r = 0.022$, $p = 0.5$), indicating weak or absent coupling between the two variables. This lack of association suggests that the amplification in $\dot{V}_E$ was not driven solely by metabolic factors but may instead reflect use-dependent sensitization of ventilatory control mechanisms.

The observed increase in ventilatory responsiveness during repeated IHc cycles may represent an early form of chemosensory gain — a feature consistent with the proposed mechanisms of sensory LTF. Prior animal studies have shown that repeated stimulation of the CSN elicits serotonin-dependent LTF of respiratory motor output (81), and that the magnitude of sensory LTF is influenced by the intensity, duration, and frequency of carotid body activation (63). Collectively, these findings underscore the evolving nature of ventilatory control during IHc, with evidence for both immediate chemoreflex engagement and progressive sensitization that may precede the emergence of sensory LTF.

Chapter 7

Perspectives

The present findings have implications for both clinical research and the broader understanding of autonomic and respiratory plasticity. First, the observation that IHc was associated with exaggerated HR responses during and following moderate-intensity exercise suggests that IHc may serve as a valuable model for investigating autonomic regulation and potential sympathetic plasticity. This could be particularly relevant for populations with dysregulated autonomic function, such as individuals with heart failure or OSA, where controlled CO_2 exposure may eventually offer therapeutic insights.

Second, the ventilatory adjustments observed – alongside the evidence of increased PHC- underscore the contribution of chemoreflex plasticity to acute ventilatory control. These findings support the need for future mechanistic studies which include direct assessments of chemoreflex fain and gas exchange to better understand how IHc influences respiratory regulation, both at rest and during exertion.

Finally, the novel combination of IHc with moderate-intensity exercise in the current protocol revealed integrated cardiovascular and ventilatory effects that may not be captured through either stimulus in isolation. Although further work is needed to isolate the additive or synergistic effects, this approach presents a promising framework for future research into conditioning protocols aimed at enhancing cardiorespiratory efficiency and adaptability in both healthy and clinical populations.

In summary, this study highlights the potential for IHc, particularly when combined with exercise, to modulate cardiovascular and ventilatory function. These results provide an early

foundation for exploring how repeated respiratory stimuli interact with physiological state to shape integrated control mechanisms in humans.

Chapter 8
Considerations and Limitations

There are limitations for this study. First was the potential unblinding of some participants. Given the participants were familiarized with IHc during Day 1 (and potentially through previous participation in studies manipulating inspired gases), some participants may have been able to distinguish whether they received IHc or control on Day 2. This could have elicited an anticipatory autonomic response on Day 3, such as increased HR, depending on perceived exposure. Similar to the known feed-forward influence of central command during anticipated exercise, this may have contributed to baseline cardiorespiratory differences between conditions despite blinding measures taken (as outlined in section *4.3.2 Days 2 and 3 Experimental Protocol)* (82).

Another potential limitation of the study relates to body positioning during recumbent cycling. Characterized by an increased hip joint angle in comparison to upright cycling, the recumbent cycling seemed to elicit an urge to void in several participants. Despite subjects being instructed to void prior to testing, this sensation was frequently reported during the 40-minute exercise bout and may have transiently elevated blood pressure via sympathetic activation. Notably, participants consistently reported that the urge subsided immediately upon cessation of exercise, even when remaining seated, indicating that the phenomenon was directly linked to the dynamic nature of cycling in relation to trunk and lower-limb angles. Importantly, this response was observed consistently across both conditions, suggesting that its potential confounding influence on cardiovascular responses was independent of the experimental intervention. Future studies should consider optimizing participant positioning or using an alternative exercise method to mitigate this effect on hemodynamic outcomes.

The calculation of $\Delta\dot{V}_E/\Delta\dot{V}CO_2$ also presented challenges. In several cases, minimal changes in $\dot{V}CO_2$ resulted in disproportionately large or physiologically implausible ratios, limiting the interpretability of these data. Future studies may address this issue by clamping $P_{ET}CO_2$ during recovery to ensure a more standardized chemoreceptor stimulus. Also, evaluating $\Delta\dot{V}_E$ in response to hyperoxia during recovery may help differentiate whether elevated $\dot{V}_E$ reflects tonic peripheral chemoreceptor input, as suppression of $\dot{V}_E$ under hyperoxia would support chemosensory contribution.

Another limitation was the limited sampling of post-condition resting data. Aside from BP, all post-condition measurements were only collected once during rest and exercise post-condition. The resting measurements occurred ~12–15 minutes post-IHc, which may not have fully captured the temporal emergence of vLTF. This is particularly relevant under the hypothesis that exercise may delay or blunt the expression of vLTF. Future protocols should incorporate multiple post-condition time points for ventilatory and autonomic measures to better characterize the time course of plasticity expression.

Finally, direct measurements of SNA, HR variability, or arterial blood gases were not included, limiting mechanistic interpretation. Although peripheral chemoreceptor activation and SNS engagement were inferred from indirect physiological markers (e.g., HR, BP, and end-tidal gases), arterial blood gases would have provided a more precise evaluation of $\dot{V}_A$ and systemic CO_2 retention. Without them, it remains uncertain whether changes in end-tidal gases fully reflected arterial gas tensions. Future studies should incorporate direct assessments, such as microneurography for SNA or continuous heart rate variability analyses, alongside arterial blood gas measurements to enhance mechanistic understanding of autonomic and ventilatory responses to IHc.

Chapter 9
Conclusion

This study investigated the effects of IHc, combined with moderate-intensity exercise, on cardiovascular function and ventilatory control in healthy adults. The presence of exercise seemingly abolished the expected elevations in resting MAP following IHc, despite responses diverging from control during exercise. Significant post-IHc increases in HR and PHC were observed, suggestive of chemosensory facilitation and altered autonomic regulation. Although ventilatory changes during exercise appeared proportionate to metabolic demand, uncoupling of $\dot{V}_E$ from $\dot{V}CO_2$ at rest may reflect early or transient expression of ventilatory plasticity. Additionally, time-dependant increases in HR and $\dot{V}_E$ during IHc, along with amplified ventilatory responses to repeated hypercapnic cycles, provide further support for progressive physiological adaptation within respiratory and autonomic circuits.

Together, these findings highlight the potential for IHc to induce state-dependent respiratory plasticity in humans, with exercise modulating both the timing and magnitude of these responses. To our knowledge, this is the first study to report key features of vLTF following IHc without concurrent hypoxia in an exercising model. These results contribute novel insight into how intermittent respiratory stimuli interact with physiological state to shape integrated ventilatory and autonomic regulation – a concept with important implications for both research and rehabilitation settings.

References

1. Vermeulen TD, Benbaruj J, Brown CV, Shafer BM, Floras JS, Foster GE. Peripheral chemoreflex contribution to ventilatory long-term facilitation induced by acute intermittent hypercapnic hypoxia in males and females. J Physiol. 2020 Oct;598(20):4713–30.

2. Griffin HS, Pugh K, Kumar P, Balanos GM. Long-term facilitation of ventilation following acute continuous hypoxia in awake humans during sustained hypercapnia. J Physiol. 2012 Oct 15;590(Pt 20):5151–65.

3. Pamenter ME, Powell FL. Signalling mechanisms of long term facilitation of breathing with intermittent hypoxia. F1000Prime Rep. 2013 Jul 1;5:23.

4. Syed Z, Lin HS, Mateika JH. The impact of arousal state, sex, and sleep apnea on the magnitude of progressive augmentation and ventilatory long-term facilitation. J Appl Physiol. 2013 Jan 1;114(1):52–65.

5. Leuenberger UA, Hogeman CS, Quraishi S, Linton-Frazier L, Gray KS. Short-term intermittent hypoxia enhances sympathetic responses to continuous hypoxia in humans. J Appl Physiol. 2007 Sep;103(3):835–42.

6. Roy A, Farnham MMJ, Derakhshan F, Pilowsky PM, Wilson RJA. Acute intermittent hypoxia with concurrent hypercapnia evokes P2X and TRPV1 receptor-dependent sensory long-term facilitation in naïve carotid bodies. J Physiol. 2018 Aug 1;596(15):3149–69.

7. Shing, C. L. H., Thrall, S. F., Lance, M. L., & Foster, G. E. (2025). The effects of acute intermittent hypercapnia on cardiovascular and ventilatory control. *Journal of Applied Physiology*, *138*(5), 1217–1227. https://doi.org/10.1152/japplphysiol.00654.2024

8. Constantini K, Bouillet AC, Wiggins CC, Martin BJ, Chapman RF. Ventilatory Responsiveness during Exercise and Performance Impairment in Acute Hypoxia. Med Sci Sports Exerc. 2021 Feb 1;53(2):295–305.

9. Yamashiro SM, Kato T, Matsumoto T. Altered chemosensitivity to CO2 during exercise. Physiol Rep. 2021 Jun;9(11):e14882.

10. Dominelli PB, Wiggins CC, Roy TK, Secomb TW, Curry TB, Joyner MJ. The Oxygen Cascade During Exercise in Health and Disease. Mayo Clin Proc. 2021 Apr;96(4):1017–32.

11. Jonz MG. Insights into the evolution of polymodal chemoreceptors. Acta Histochem. 2018 Oct;120(7):623–9.

12. Dempsey JA, Powell FL, Bisgard GE, Blain GM, Poulin MJ, Smith CA. Role of chemoreception in cardiorespiratory acclimatization to, and deacclimatization from, hypoxia. J Appl Physiol. 2014 Apr 1;116(7):858–66.

13. O'Regan RG, Majcherczyk S. Role of peripheral chemoreceptors and central chemosensitivity in the regulation of respiration and circulation. J Exp Biol. 1982 Oct;100:23–40.

14. Iturriaga R, Alcayaga J, Chapleau MW, Somers VK. Carotid body chemoreceptors: physiology, pathology, and implications for health and disease. Physiol Rev. 2021 Jul 1;101(3):1177–235.

15. Daly M de B, Scott MJ. The effects of stimulation of the carotid body chemoreceptors on heart rate in the dog. J Physiol. 1958 Nov 10;144(1):148–66.

16. Nattie E, Li A. Central Chemoreceptors: Locations and Functions. Compr Physiol. 2012 Jan;2(1):221–54.

17. Haldane JS, Priestley JG. The regulation of the lung-ventilation. J Physiol. 1905 May 9;32(3–4):225–66.

18. Guyenet PG, Stornetta RL, Bayliss DA. Central respiratory chemoreception. J Comp Neurol. 2010 Oct 1;518(19):3883–906.

19. Pamenter ME, Powell FL. Time Domains of the Hypoxic Ventilatory Response and Their Molecular Basis. Compr Physiol. 2016 Jun 13;6(3):1345–85.

20. Steinback CD, Poulin MJ. Ventilatory responses to isocapnic and poikilocapnic hypoxia in humans. Respir Physiol Neurobiol. 2007 Feb 15;155(2):104–13.

21. Heinonen IHA, Boushel R, Kalliokoski KK. The Circulatory and Metabolic Responses to Hypoxia in Humans – With Special Reference to Adipose Tissue Physiology and Obesity. Front Endocrinol. 2016 Aug 29;7:116.

22. Faulhaber M, Gatterer H, Haider T, Linser T, Netzer N, Burtscher M. Heart rate and blood pressure responses during hypoxic cycles of a 3-week intermittent hypoxia breathing program in patients at risk for or with mild COPD. Int J Chron Obstruct Pulmon Dis. 2015 Feb 11;10:339–45.

23. Siebenmann C, Lundby C. Regulation of cardiac output in hypoxia. Scand J Med Sci Sports. 2015 Dec;25 Suppl 4:53–9.

24. Price HL. EFFECTS OF CARBON DIOXIDE ON THE CARDIOVASCULAR SYSTEM. Anesthesiology. 1960 Nov 1;21(6):652–63.

25. Gheshmy A, Anari A, Besada D, Reid SG. Afferent input modulates the chronic hypercapnia-induced increase in respiratory-related central pH/CO2 chemosensitivity in the cane toad (Bufo marinus). J Exp Biol. 2007 Jan;210(Pt 2):227–37.

26. Cullen DJ, Eger EI. Cardiovascular effects of carbon dioxide in man. Anesthesiology. 1974 Oct;41(4):345–9.

27. Babb TG. Ventilatory response to exercise in subjects breathing CO2 or HeO2. J Appl Physiol Bethesda Md 1985. 1997 Mar;82(3):746–54.

28. Ryan BJ, Seeley AD, Pitsas DM, Mayer TA, Caldwell AR, Ceaser TG, et al. Influence of graded hypercapnia on endurance exercise performance in healthy humans. Am J Physiol-Regul Integr Comp Physiol. 2022 Nov;323(5):R638–47.

29. Moriyama S, Ichinose M, Dobashi K, Matsutake R, Sakamoto M, Fujii N, et al. Hypercapnia elicits differential vascular and blood flow responses in the cerebral circulation and active skeletal muscles in exercising humans. Physiol Rep. 2022 Apr 24;10(8):e15274.

30. Bavis RW, Mitchell GS. Intermittent hypoxia induces phrenic long-term facilitation in carotid-denervated rats. J Appl Physiol Bethesda Md 1985. 2003 Jan;94(1):399–409.

31. Kim SJ, Fong AY, Pilowsky PM, Abbott SBG. Sympathoexcitation following intermittent hypoxia in rat is mediated by circulating angiotensin II acting at the carotid body and subfornical organ. J Physiol. 2018 Aug;596(15):3217–32.

32. Foster GE, McKenzie DC, Milsom WK, Sheel AW. Effects of two protocols of intermittent hypoxia on human ventilatory, cardiovascular and cerebral responses to hypoxia. J Physiol. 2005 Sep 1;567(Pt 2):689–99.

33. Katayama K, Sato K, Matsuo H, Hotta N, Sun Z, Ishida K, et al. Changes in ventilatory responses to hypercapnia and hypoxia after intermittent hypoxia in humans. Respir Physiol Neurobiol. 2005 Mar;146(1):55–65.

34. Harris DP, Balasubramaniam A, Badr MS, Mateika JH. Long-term facilitation of ventilation and genioglossus muscle activity is evident in the presence of elevated levels of carbon dioxide in awake humans. Am J Physiol-Regul Integr Comp Physiol. 2006 Oct;291(4):R1111–9.

35. Foster GE, Hanly PJ, Ahmed SB, Beaudin AE, Pialoux V, Poulin MJ. Intermittent Hypoxia Increases Arterial Blood Pressure in Humans Through a Renin-Angiotensin System-Dependent Mechanism. Hypertension. 2010 Sep;56(3):369–77.

36. Lusina SJC, Kennedy PM, Inglis JT, McKenzie DC, Ayas NT, Sheel AW. Long-term intermittent hypoxia increases sympathetic activity and chemosensitivity during acute hypoxia in humans. J Physiol. 2006 Sep 15;575(Pt 3):961–70.

37. Turnbull CD. Intermittent hypoxia, cardiovascular disease and obstructive sleep apnoea. J Thorac Dis [Internet]. 2018 Jan [cited 2023 Dec 28];10(Suppl 1). Available from: https://jtd.amegroups.org/article/view/17157

38. Pianosi P, Khoo MCK. Change in the peripheral CO2 chemoreflex from rest to exercise. Eur J Appl Physiol. 1995 Jul 1;70(4):360–6.

39. Miyamoto T, Sotobayashi D, Ito G, Kawai E, Nakahara H, Ueda S, et al. Physiological role of anticipatory cardiorespiratory responses to exercise. Physiol Rep. 2022 Mar 5;10(5):e15210.

40. Rowell LB, O'Leary DS. Reflex control of the circulation during exercise: chemoreflexes and mechanoreflexes. J Appl Physiol Bethesda Md 1985. 1990 Aug;69(2):407–18.

41. Standardization of Spirometry, 1994 Update. American Thoracic Society. Am J Respir Crit Care Med. 1995 Sep;152(3):1107–36.

42. Niemel K, Palatsi I, Linnaluoto M, Takkunen J. Criteria for maximum oxygen uptake in progressive bicycle tests. Eur J Appl Physiol. 1980 Jun 1;44(1):51–9.

43. Mann L, Chan J, Angus S, Doherty C, Thompson B, Foster G, et al. Peripheral hypercapnic chemosensitivity in trained and untrained females and males during exercise. J Appl Physiol Bethesda Md 1985. 2022 Oct 27;133.

44. Stuckless TJR, Vermeulen TD, Brown CV, Boulet LM, Shafer BM, Wakeham DJ, et al. Acute intermittent hypercapnic hypoxia and sympathetic neurovascular transduction in men. J Physiol. 2020;598(3):473–87.

45. Smith KJ, Wildfong KW, Hoiland RL, Harper M, Lewis NC, Pool A, et al. Role of CO2 in the cerebral hyperemic response to incremental normoxic and hyperoxic exercise. J Appl Physiol. 2016 Apr 15;120(8):843–54.

46. Mann L. The Difference in Peripheral Chemosensitivity Between Trained and Untrained Individuals during Exercise [Internet] [Master Thesis]. University of Waterloo; 2022 [cited 2024 Jan 3]. Available from: https://uwspace.uwaterloo.ca/handle/10012/17854

47. R Core Team. R Foundation for Statistical Computing. 2021 [cited 2023 Aug 14]. R: The R Project for Statistical Computing. Available from: https://www.r-project.org/

48. Dick, T. E., Hsieh, Y.-H., Wang, N., & Prabhakar, N. (2007). Acute intermittent hypoxia increases both phrenic and sympathetic nerve activities in the rat. *Experimental Physiology*, *92*(1), 87–97.

49. Vose, A. K., Welch, J. F., Nair, J., Dale, E. A., Fox, E. J., Muir, G. D., Trumbower, R. D., & Mitchell, G. S. (2022). Therapeutic acute intermittent hypoxia: A translational roadmap for spinal cord injury and neuromuscular disease. *Experimental Neurology*, *347*, 113891.

50. Hoffman, M. S., Nichols, N. L., Macfarlane, P. M., & Mitchell, G. S. (2012). Phrenic long-term facilitation after acute intermittent hypoxia requires spinal ERK activation but not TrkB synthesis. *Journal of Applied Physiology*, *113*(8), 1184–1193.

51. Prabhakar, N. R., & Kumar, G. K. (2010). Mechanisms of Sympathetic Activation and Blood Pressure Elevation by Intermittent Hypoxia. *Respiratory Physiology & Neurobiology*, *174*(1–2), 156–161.

52. Xing, T., Pilowsky, P. M., & Fong, A. Y. (2014). Mechanism of sympathetic activation and blood pressure elevation in humans and animals following acute intermittent hypoxia. *Progress in Brain Research*, *209*, 131–146.

53. Kim, S. J., Kim, Y. J., Kakall, Z., Farnham, M. M. J., & Pilowsky, P. M. (2016). Intermittent hypoxia-induced cardiorespiratory long-term facilitation: A new role for microglia. *Respiratory Physiology & Neurobiology*, *226*, 30–38.

54. Hoffman, M. S., Nichols, N. L., Macfarlane, P. M., & Mitchell, G. S. (2012). Phrenic long-term facilitation after acute intermittent hypoxia requires spinal ERK activation but not TrkB synthesis. *Journal of Applied Physiology*, *113*(8), 1184–1193.

55. Sleiman, S. F., Henry, J., Al-Haddad, R., El Hayek, L., Abou Haidar, E., Stringer, T., Ulja, D., Karuppagounder, S. S., Holson, E. B., Ratan, R. R., Ninan, I., & Chao, M. V. (n.d.). Exercise promotes the expression of brain derived neurotrophic factor (BDNF) through the action of the ketone body β-hydroxybutyrate. *eLife*, *5*, e15092.

56. Welch, J. F., Nair, J., Argento, P. J., Mitchell, G. S., & Fox, E. J. (2022). Acute intermittent hypercapnic-hypoxia elicits central neural respiratory motor plasticity in humans. *The Journal of Physiology*, *600*(10), 2515–2533.

57. Cevese, A. (2005). Coronary circulation: Nitric oxide and hypercapnic acidosis. *Cardiovascular Research*, *66*(1), 7–8.

58. A. Ruivo, J., & Alcântara, P. (2012). Hypertension and exercise. *Revista Portuguesa de Cardiologia (English Edition)*, *31*(2), 151–158.

59. Willie, C. K., Ainslie, P. N., Taylor, C. E., Jones, H., Sin, P. Y. W., & Tzeng, Y.-C. (2011). Neuromechanical Features of the Cardiac Baroreflex After Exercise. *Hypertension*, *57*(5), 927–933.

60. Cooper, V. L., Pearson, S. B., Bowker, C. M., Elliott, M. W., & Hainsworth, R. (2005). Interaction of chemoreceptor and baroreceptor reflexes by hypoxia and hypercapnia – a mechanism for promoting hypertension in obstructive sleep apnoea. *The Journal of Physiology*, *568*(2), 677–687.

61. Yamashiro, S. M., Kato, T., & Matsumoto, T. (2024). Modeling Long-Term Facilitation of Respiration During Interval Exercise in Humans. *Annals of Biomedical Engineering*, *52*(2), 250–258.

62. Prabhakar, N. R., Dick, T. E., Nanduri, J., & Kumar, G. K. (2007). Systemic, cellular and molecular analysis of chemoreflex-mediated sympathoexcitation by chronic intermittent hypoxia. *Experimental Physiology*, *92*(1), 39–44.

63. Peng, Y.-J., Overholt, J. L., Kline, D., Kumar, G. K., & Prabhakar, N. R. (2003). Induction of sensory long-term facilitation in the carotid body by intermittent hypoxia: Implications for recurrent apneas. *Proceedings of the National Academy of Sciences*, *100*(17), 10073–10078.

64. Kumar, P., & Prabhakar, N. R. (2012). Peripheral Chemoreceptors: Function and Plasticity of the Carotid Body. In *Comprehensive Physiology* (pp. 141–219). John Wiley & Sons, Ltd.

65. Teppema, L. J., & Dahan, A. (2010). The Ventilatory Response to Hypoxia in Mammals: Mechanisms, Measurement, and Analysis. *Physiological Reviews*, *90*(2), 675–754.

66. Peng, Y.-J., & Prabhakar, N. R. (2004). Effect of two paradigms of chronic intermittent hypoxia on carotid body sensory activity. *Journal of Applied Physiology*, *96*(3), 1236–1242.

67. Prabhakar, N. R. (2011). SENSORY PLASTICITY OF THE CAROTID BODY: ROLE OF REACTIVE OXYGEN SPECIES AND PHYSIOLOGICAL SIGNIFICANCE. *Respiratory Physiology & Neurobiology*, *178*(3), 375–380.

68. Willie, C. K., Ainslie, P. N., Taylor, C. E., Jones, H., Sin, P. Y. W., & Tzeng, Y.-C. (2011). Neuromechanical Features of the Cardiac Baroreflex After Exercise. *Hypertension*, *57*(5), 927–933.

69. Potts, J. T., Fong, A. Y., Anguelov, P. I., Lee, S., McGovern, D., & Grias, I. (2007). Targeted deletion of neurokinin-1 receptor expressing nucleus tractus solitarii neurons precludes somatosensory depression of arterial baroreceptor-heart rate reflex. *Neuroscience*, *145*(3), 1168–1181.

70. Fuller, D. D., Johnson, S. M., Olson, E. B., & Mitchell, G. S. (2003). Synaptic Pathways to Phrenic Motoneurons Are Enhanced by Chronic Intermittent Hypoxia after Cervical Spinal Cord Injury. *The Journal of Neuroscience*, *23*(7), 2993–3000.

71. Bach, K. B., & Mitchell, G. S. (1996). Hypoxia-induced long-term facilitation of respiratory activity is serotonin dependent. *Respiration Physiology*, *104*(2), 251–260.

72. Martinez, D., Rogers, R. C., Hasser, E. M., Hermann, G. E., & Kline, D. D. (2020). Loss of excitatory amino acid transporter restraint following chronic intermittent hypoxia contributes to synaptic alterations in nucleus tractus solitarii. *Journal of Neurophysiology*, *123*(6), 2122–2135.

73. Halliwill, J. R. (2001). Mechanisms and clinical implications of Post-Exercise hypotension in humans. *Exercise and Sport Sciences Reviews*, *29*(2), 65–70.

74. Bhogal, A. S., & Mani, A. R. (2017). Pattern Analysis of Oxygen Saturation Variability in Healthy Individuals: Entropy of Pulse Oximetry Signals Carries Information about Mean Oxygen Saturation. *Frontiers in Physiology*, *8*, 555.

75. Powell, F. L. (2007). The influence of chronic hypoxia upon chemoreception. *Respiratory Physiology & Neurobiology*, *157*(1), 154–161.

76. Guyenet, P. G. (2014). Regulation of Breathing and Autonomic Outflows by Chemoreceptors. *Comprehensive Physiology*, *4*(4), 1511–1562.

77. Rio, R. D., Moya, E. A., & Iturriaga, R. (2010). Carotid body and cardiorespiratory alterations in intermittent hypoxia: The oxidative link. *European Respiratory Journal*, *36*(1), 143–150.

78. Kaufman, M. P., & Hayes, S. G. (2002). The Exercise Pressor Reflex. *Clinical Autonomic Research*, *12*(6), 429–439.

79. Stickland, M. K., Miller, J. D., Smith, C. A., & Dempsey, J. A. (2007). Carotid chemoreceptor modulation of regional blood flow distribution during exercise in health and chronic heart failure. *Circulation Research*, *100*(9), 1371–1378.

80. Kline, D. D., Ramirez-Navarro, A., & Kunze, D. L. (2007). Adaptive Depression in Synaptic Transmission in the Nucleus of the Solitary Tract after *In Vivo* Chronic Intermittent Hypoxia: Evidence for Homeostatic Plasticity. *The Journal of Neuroscience*, *27*(17), 4663–4673.

81. Fregosi, R. F., & Mitchell, G. S. (1994). Long-term facilitation of inspiratory intercostal nerve activity following carotid sinus nerve stimulation in cats. *The Journal of Physiology*, *477*(Pt 3), 469–479.

82. Miyamoto, T., Sotobayashi, D., Ito, G., Kawai, E., Nakahara, H., Ueda, S., Toyama, T., Saku, K., Nakanishi, Y., & Kinoshita, H. (2022). Physiological role of anticipatory cardiorespiratory responses to exercise. *Physiological Reports*, *10*(5), e15210.

83. Golder, F. J., & Mitchell, G. S. (2005). Spinal Synaptic Enhancement with Acute Intermittent Hypoxia Improves Respiratory Function after Chronic Cervical Spinal Cord Injury. *Journal of Neuroscience*, *25*(11), 2925–2932. https://doi.org/10.1523/JNEUROSCI.0148-05.2005

84. Tessema, B., Sack, U., König, B., Serebrovska, Z., & Egorov, E. (2022). Effects of Intermittent Hypoxia in Training Regimes and in Obstructive Sleep Apnea on Aging Biomarkers and Age-Related Diseases: A Systematic Review. *Frontiers in Aging Neuroscience*, *14*. https://doi.org/10.3389/fnagi.2022.878278

85. Shing, C., Thrall, S., Lance, M., Bird, J., Shafer, B., Soltani, M., & Foster, G. (2023). The Effects of Acute Intermittent Hypercapnia on Ventilatory and Cardiovascular Plasticity. *Physiology*, *38*(S1), 5731586. https://doi.org/10.1152/physiol.2023.38.S1.5731586